Recovery from disturbance requires resynchronization of ecosystem nutrient cycles

E. B. Rastetter,[1,8] R. D. Yanai,[2] R. Q. Thomas,[3] M. A. Vadeboncoeur,[4] T. J. Fahey,[5] M. C. Fisk,[6] B. L. Kwiatkowski,[1] and S. P. Hamburg[7]

[1]*The Ecosystems Center, Marine Biological Laboratory, 7 MBL Street, Woods Hole, Massachusetts 02543 USA*
[2]*College of Environmental Science and Forestry, State University of New York, Syracuse, New York 13210 USA*
[3]*Department of Ecology and Evolutionary Biology, Cornell University, Ithaca, New York 14853 USA*
[4]*Earth Systems Research Center, Institute for the study of Earth, Oceans, and Space, University of New Hampshire, Durham, New Hampshire 03824 USA*
[5]*Department of Natural Resources, Cornell University, Ithaca, New York 14853 USA*
[6]*Department of Zoology, Miami University, Oxford, Ohio 45056 USA*
[7]*Environmental Defense Fund, Boston, Massachusetts 02108 USA*

Abstract. Nitrogen (N) and phosphorus (P) are tightly cycled in most terrestrial ecosystems, with plant uptake more than 10 times higher than the rate of supply from deposition and weathering. This near-total dependence on recycled nutrients and the stoichiometric constraints on resource use by plants and microbes mean that the two cycles have to be synchronized such that the ratio of N:P in plant uptake, litterfall, and net mineralization are nearly the same. Disturbance can disrupt this synchronization if there is a disproportionate loss of one nutrient relative to the other. We model the resynchronization of N and P cycles following harvest of a northern hardwood forest. In our simulations, nutrient loss in the harvest is small relative to postharvest losses. The low N:P ratio of harvest residue results in a preferential release of P and retention of N. The P release is in excess of plant requirements and P is lost from the active ecosystem cycle through secondary mineral formation and leaching early in succession. Because external P inputs are small, the resynchronization of the N and P cycles later in succession is achieved by a commensurate loss of N. Through succession, the ecosystem undergoes alternating periods of N limitation, then P limitation, and eventually co-limitation as the two cycles resynchronize. However, our simulations indicate that the overall rate and extent of recovery is limited by P unless a mechanism exists either to prevent the P loss early in succession (e.g., P sequestration not stoichiometrically constrained by N) or to increase the P supply to the ecosystem later in succession (e.g., biologically enhanced weathering). Our model provides a heuristic perspective from which to assess the resynchronization among tightly cycled nutrients and the effect of that resynchronization on recovery of ecosystems from disturbance.

Key words: co-limitation; disturbance; ecosystem succession; N:P ratio; nutrient cycles; nutrient limitation; resource optimization; stoichiometric constraints; terrestrial ecosystem cycling.

INTRODUCTION

Nitrogen (N) and phosphorus (P) are tightly held by most terrestrial ecosystems and are repeatedly recycled within the ecosystem. External sources of these nutrients from weathering and atmospheric deposition are only a small component of the overall nutrient budget, supplying less than a 10th of plant requirements in a mature ecosystem. For example, even with elevated anthropogenic N deposition, N inputs to the Hubbard Brook Experimental Forest in central New Hampshire, USA are <6% of the gross annual N uptake by plants (Whittaker et al. 1979, Ollinger et al. 1993). For P, deposition and primary and secondary mineral weath-

ering at Hubbard Brook are equivalent to <1% of the P uptake by plants (Yanai 1992).

This near-total dependence on recycled nutrients and the stoichiometric constraints on plants and microbes mean that the cycles of N and P (and other tightly recycled nutrients) have to be closely synchronized in the ecosystem, at least in the steady state. Here we define "synchrony" in terms of the cycling of nutrients from inorganic soil nutrients to vegetation to soil organic matter and associated microbes back to the inorganic soil nutrients. At a steady state for any nutrient with a fully closed cycle (i.e., no inputs to or losses from the ecosystem), uptake by vegetation, nutrient loss in litter, and net mineralization all have to be equal on an annual time scale. The cycles of any two such nutrients have to be fully synchronized in the sense that the ratio of the two nutrients would be the same for all of these fluxes. As long as the inputs of N and P to the ecosystem

remain small relative to their internal cycling rate, the two cycles will be synchronized to one another. We hypothesize that this synchronization results in co-limitation by N and P as the ecosystem matures and explains why co-limitation by N and P appears to be common among ecosystems globally (Davidson and Howarth 2007, Elser et al. 2007), including temperate forests that have been widely viewed as N limited (Naples and Fisk 2010, Vadeboncoeur 2010).

This synchrony can be disrupted by disturbance if, for example, the disturbance results in a proportionally higher loss of one nutrient relative to the other tightly cycled nutrients. Following such a disturbance, both plants and microbes would be expected to optimize resource acquisition to maintain their required stoichiometry (Bloom et al. 1985, Chapin et al. 1987, Rastetter et al. 1997), which would act to retain limiting nutrients in the ecosystem but could allow more abundant nutrients to accumulate in forms susceptible to loss from the ecosystem. We therefore hypothesize that the desynchronization of nutrient cycling results in post-disturbance losses of the more rapidly cycling nutrients and that the responses of plants and microbes to limitation by the more slowly cycling nutrients will exacerbate the loss of the rapidly cycling nutrients.

Synchronization among nutrient cycles and the response of plants and microbes to disruptions to that synchrony should also have important implications for forest management. One of the key objectives of forest management is to maintain long-term site fertility. If our hypothesis is corroborated, then effective management strategies should be developed to resynchronize nutrient cycles soon after a disturbance and to time mitigation strategies to correspond to the pattern in relative limitation by tightly cycling nutrients.

Approach

Because of the complexity of interactions among nutrient cycles and the long recovery time for most ecosystems, it is difficult to examine post-disturbance resynchronization of nutrient cycles with a purely empirical approach. We therefore apply a model parameterized to the extensive data sets from the Hubbard Brook Experimental Forest. Our aim is to develop a heuristic perspective from which to assess our hypotheses about the resynchronization among tightly cycled nutrients and to help unravel the complexities in ecosystem nutrient cycles (Bernal et al. 2012) and how they respond to disturbance.

We use version IV of the Multiple Element Limitation (MEL) model, which couples ecosystem C, N, P, and water cycles. The heart of this model, and what sets it apart from most ecosystem models, is a dynamic algorithm that simulates the redistribution of plant "uptake effort" to optimize the relative acquisition of resources from the environment (Rastetter et al. 1997, 2001, Rastetter 2011). The uptake effort is an aggregate representation of all plant assets (biomass, enzymes,

carbohydrate, and so forth) that can be deployed toward acquiring resources. In addition, from the aggregated-vegetation perspective of the MEL model, the reallocation of uptake assets would also represent shifts in the plant community toward species with characteristics that are better adapted to current conditions. The model includes a similar optimization for soil microbes, but this optimization is imposed instantaneously rather than through a dynamic algorithm. Our analysis is restricted to an analysis of post-disturbance recovery to the original state of the forest and therefore does not assess the potential for transitions to alternative stable states (May 1977, Beisner et al. 2003).

We examine a base simulation plus eight sets of simulations designed to assess model sensitivity to ecosystem characteristics identified as important in the analysis of the base simulation.

1) *Base simulation.*—In our base simulation we analyze biomass recovery, soil dynamics, and changes in N and P cycles as they resynchronize following a bole-only harvest.

2) *Constant distribution of uptake effort.*—To assess the importance of the optimization of uptake effort, we examine the bole-only simulation with the distribution of uptake effort held constant at the initial and steady-state distributions and at several intermediate distributions from the base simulations.

3) *Post-disturbance organic residue.*—To assess the importance of the initial nutrient removal and post-disturbance nutrient immobilization by the organic residue, we simulate a whole-tree harvest (most biomass removed) and a hurricane blowdown (no biomass removed).

4) *Buffered NH_4^+ and PO_4^{3-}.*—To assess the importance of post-disturbance nutrient losses, we inhibit the buildup of NH_4^+ and PO_4^{3-} in soil solution, and hence inhibit losses through leaching, denitrification, and secondary P mineral formation, by increasing the exchange affinity of soils for these ions, both individually and in combination (increased E_{NH4} and ε_{NH4} and/or E_{PO4}, and ε_{PO4}; Appendix: Table A1, Eqs. A.23 and A.26).

5) *Coarse woody debris turnover.*—To assess the importance of soil immobilization potential for retaining nutrients following a disturbance, we alter the supply of C-rich, nutrient-poor substrate to soil microbes by simulating forest recovery with coarse woody debris turnover rates half the rates in the base simulation (doubled D_{Cc}, D_{Nc}, and D_{Pc}, and halved r_{CW} in the Appendix: Table A1, Eqs. A.97–A.99).

6) *Post-disturbance replanting.*—To assess the importance of the initial nutrient uptake potential of vegetation, we simulate recovery starting with 10% of the initial biomass rather than 1%.

7) *Altered ratio of gross:net mineralization.*—To assess the importance of plant–microbe competition for nutrients, we double or halve the gross mineraliza-
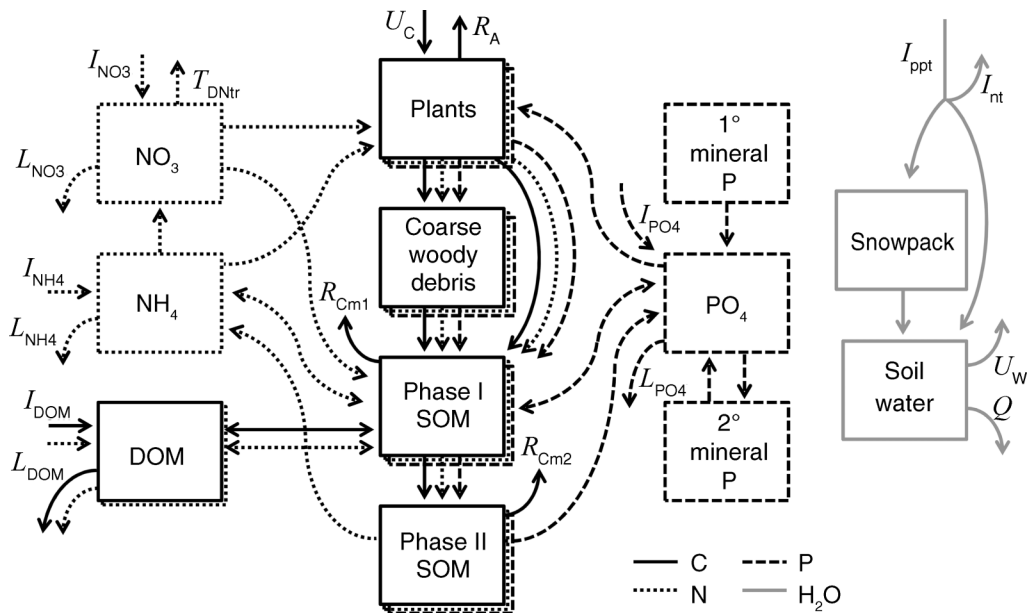
FIG. 1. The multiple element limitation (MEL) model. C, N, P, and water stocks and fluxes are distinguished respectively by solid, dotted, dashed, and gray lines. Two-headed arrows indicate fluxes in both directions. Mineral P is shown as primary (1°) and secondary (2°). For clarity, only external fluxes have been labeled: U_C, photosynthesis; R_A, autotrophic respiration; R_{Cm1} and R_{Cm2}, heterotrophic respiration from Phase I and Phase II soil organic matter (SOM); I_i, inputs of i; L_i, leaching loss of i; T_{DNtr}, denitrification; DOM, dissolved organic matter; I_{ppt}, precipitation; I_{nt}, evaporation of intercepted water; U_W, water uptake and transpiration; Q, runoff and deep percolation.

tion rates of NH_4^+ and/or PO_4^{3-}, but leave the steady-state net mineralization rates unchanged (altered α_{NH4}, α_{PO4}, ψ_{Nm}, and ψ_{Pm}; Appendix: Table A1, Eqs. A.102, A.104, A.106, and A.107).

8) *Distribution of N and P between Phase I and Phase II (Melillo et al. 1989) soil organic matter (SOM) pools.*—To assess the importance of soil nutrient turnover rates, we redistribute N and P between Phase I SOM, which turns over more quickly, and Phase II SOM, which is more recalcitrant (altered ϕ_N, ϕ_P, α_{NH4}, α_{NO3}, α_{PO4}, ψ_m, ψ_{Nm}, ψ_{Pm}, and r_{DOM} in the Appendix: Table A1, Eqs. A.102–A.115).

9) *NH_4^+ and PO_4^{3-} fertilization.*—To assess the effects of active acquisition of external sources of N and P (e.g., N-fixation, biologically mediated weathering) and to assess potential mitigation strategies based on nutrient addition, we simulate fertilizations with NH_4^+ and PO_4^{3-}, individually and in combination, at different stages of the recovery. Details on how these simulations were implemented follow.

THE MULTIPLE ELEMENT LIMITATION (MEL) MODEL

Version IV of the MEL model couples ecosystem C, N, P, and water cycles and runs on a daily time step (Fig. 1; see Appendix). We use an aggregate representation of vegetation, partitioned allometrically into woody and active biomass (Appendix: Eqs. A.35–A.36). The algorithm that redistributes uptake effort allocates the active biomass to leaves or fine roots based on the relative limitation by canopy vs. soil resources (Rastetter et al. 2001; Appendix: Eqs. A.37–A.38). Canopy expansion is proportional to the springtime degree-day sum, but leaf-fall timing is prescribed (Appendix: Eq. A.45). We assume a constant turnover of wood and roots throughout the year (Appendix: Eq. A.70). Photosynthesis is co-limited by CO_2, light, and water (Appendix: Eqs. A.46–A.60). Nutrient uptake follows Michaelis-Menten kinetics with the substrate concentration at the root set by a balance between uptake and nutrient diffusion through the soil and maximum uptake set by the expended effort (Appendix: Eqs. A.64–A.68).

We use uptake effort to represent the aggregate of all plant assets (such as biomass, enzymes, carbohydrate) that can be deployed toward the acquisition of resources. The abundance of these assets increases in proportion to the active biomass in the vegetation and the dynamic allocation algorithm calculates the fraction of these uptake assets (V_i) allocated toward acquiring each resource (Appendix: Eqs. A.75–A.95); see Rastetter (2011). Uptake is proportional to both V_i and the total amount of active biomass.

The allocation of effort is based on the current requirements for, and the current uptake rates of, the resources. The requirement for each resource equals its consumption in metabolism plus its loss in tissue turnover times a factor that compensates for deviations of the resource concentrations in biomass from an

optimum concentration (Appendix: Eqs. A.76–A.78). We calculate this optimum concentration from the allometric distribution of biomass among tissues and parameters defining the optimum concentrations in the tissues (parameters q_{LN}, q_{WN}, q_{RN}, q_{LP}, q_{WP}, and q_{RP}, where q is the biomass optimum of N or P (subscripts) in leaves, woody tissues, and roots (subscripts L, W, and R, respectively); see Appendix: Table A1, Eqs. A.43–A.44 and Table A2, definitions). The dynamic resource optimization scheme allocates uptake effort among resources based on a function Ω_i that increases monotonically with the ratio of resource requirement to resource uptake (Appendix: Eqs. A.88–A.94):

$$dV_i/dt = a \ln (\Phi\Omega_i)V_i$$

$$\Phi = \prod_{j=1}^{n}(\Omega_j)^{-V_j} \qquad (1)$$

where V_i is the fraction of uptake effort allocated toward resource i, a is an acclimation rate parameter (day^{-1}), and Φ is a variable that is calculated to ensure that the dV_i/dt sum to zero and thereby keeps the sum of the V_i equal to 1. This allocation scheme drives the system toward a state where the ratios of uptake to requirement are equal for all resources and are in that sense equally limiting (i.e., $\Omega_i = 1/\Phi$ for all i; Bloom et al. 1985).

For the substitutable resources NH_4^+ and NO_3^-, we calculate the requirement for each based on the total N requirements and the marginal yield from allocated effort, including the photosynthetic effort needed to produce the energy for NO_3^- reduction (Appendix: Eqs. A.81–A.87):

$$y_{NH4} = \frac{dU_{NH4}}{dV_{NH4}}$$

$$y_{NO3} = \frac{dU_{NO3}/dV_{NO3}}{1 + dU_{NO3}/dV_{NO3}\left(\phi(dU_{CO2}/dV_{Ps})^{-1}\right)} \qquad (2)$$

where y_i is the marginal yield for resource i, U_i is the uptake of resource i, ϕ is the amount of photosynthate consumed in the uptake and assimilation of NO_3^-, and V_{Ps} is the total effort allocated toward photosynthesis (i.e., toward CO_2, light, and water). To optimize resource acquisition, the allocation of effort is toward the resource with the higher marginal yield.

We partition detritus into Phase I and Phase II soil organic matter (Melillo et al. 1989) and coarse woody debris. Coarse woody debris serves as a lag storage that is slowly (~10-yr C turnover) converted to Phase I SOM and subsequently decomposes or is converted to Phase II material (Hyvönen and Ågren 2001). Phase I SOM represents the young, more active organic matter that implicitly includes microbial biomass, both mineralizes and immobilizes nutrients, and has a relatively high respiration rate (~7-yr C turnover; Appendix: Eqs. A.96–A.114). Phase I material also converts to Phase II material at a rate that at steady state is equivalent to ~20% of the C litter flux (i.e., 20% of the initial litter is eventually converted to Phase II material; Melillo et al. 1989; Appendix: Eqs. A.117–A.119). Phase II SOM does not immobilize nutrients, but continues to mineralize nutrients and respire C at a slow rate (~113-yr C turnover; Appendix: Eqs. A.120–A.122).

Nitrogen enters the ecosystem via deposition of NH_4^+, NO_3^-, and dissolved organic N (DON). N fixation is not a major contributor to the N budgets in these forests (Likens and Bormann 1995, Bernal et al. 2012). Phosphorus enters as PO_4^{3-} via deposition or the weathering of primary and secondary P minerals (Appendix: Eqs. A.125–A.127). Nitrogen is mineralized from both Phase I and Phase II material into NH_4^+. We partition the NH_4^+ into adsorbed and dissolved fractions using a Langmuir isotherm (Weatherley and Miladinovic 2004; Appendix: Eq. A.23); rates of leaching, nitrification, and uptake by plants and microbes are calculated based on the dissolved fraction. We assume no NO_3^- sorption by soils (Nodvin et al. 1986, Kaiser and Zech 1996) and that all the NO_3^- is therefore dissolved in soil water and is available for uptake by plants and microbes, leaching, and denitrification (Appendix: Eq. A.24). DON produced from the Phase I material is partitioned between dissolved and adsorbed fractions using a Langmuir isotherm (Appendix: Eq. A.25), and the rates of microbial uptake and leaching are calculated based on the dissolved fraction. Phosphate is mineralized from both Phase I and Phase II material, partitioned between dissolved and adsorbed fraction using the Langmuir isotherm (Appendix: Eq. A.26), and the dissolved fraction is used to calculate the formation of secondary P minerals, leaching, and uptake by plants and microbes.

We partition precipitation into intercepted water, snow, and rain (Appendix: Eqs. A.134–A.135). We calculate a maximum potential intercepted volume based on the leaf area plus the surface area of the aboveground woody biomass (Appendix: Eq. A.133). We assume that all precipitation up to this maximum volume is intercepted and evaporates. Precipitation in excess of this maximum value is added either to the snow pack or to the soil water, depending on air temperature (Brubaker et al. 1996). We calculate snowmelt based on net radiation to the snowpack and air temperature (Brubaker et al. 1996; Appendix: Eq. A.137). Runoff from the soil water is proportional to the volume of water in excess of field capacity (Appendix: Eq. A.128). Soil water potential is calculated based on equations from Clapp and Hornberger (1978; Appendix: Eqs. A.28–A.32). We calculate soil water uptake and transpiration by plants as proportional to the soil water potential above the wilting potential and proportional to an index of the daily vapor pressure deficit; the proportionality is set by the allocation of effort toward water uptake in the resource optimization scheme (Appendix: Eqs. A.46–A.60).

TABLE 1. Multiple element limitation (MEL) model state variables.

State variable	Carbon (g C/m^2)			Nitrogen (g N/m^2)			Phosphorus (g P/m^2)		
	Term	Value	Source and notes	Term	Value	Source and notes	Term	Value	Source and notes
Vegetation	B_C	12 006	1	B_N	80.64	1, tissues sum: C; 4, C:N for leaves and wood; 5, root %N	B_P	10.94	1, tissues sum: C; 4, C:P for leaves, wood, and roots
CWD	D_{Cc}	1 313	1	D_{Nc}	5.80	1, C; 6, N/dry mass; assumes dry mass is 45% C	D_{Pc}	0.51	D_{Nc}; 4, dead branch P/dead branch N
Phase I SOM	D_{C1}	2 970	1, organic horizons	D_{N1}	130.72	1, C; 4, C:N surface litter + fermentation layer	D_{P1}	6.83	1, C; 4, C:P surface litter + fermentation layer
Phase II SOM	D_{C2}	12 770	1, total SOM minus organic horizons	D_{N2}	724.13	1, C; 4, C:N humus layer	D_{P2}	47.89	1, C; 4, C:P humus layer
DOC	E_{DOM}	105	2, solution DOC; 3, isotherm						
DON					3.93	E_{DOM}, this table; DOM C:N ratio, Appendix: Table A2			
NH$_4^+$				E_{NH4}	0.80	2; 7, isotherm; soil water at field capacity			
NO$_3^-$				E_{NO3}	0.03	2, soil water at field capacity			
PO$_4^{3-}$							E_{PO4}	0.081	8
Primary mineral P							P_A	69	8
Secondary minerals							P_{2nd}	39.4	8

Note: State variable abbreviations are: CWD, coarse woody debris; SOM, soil organic matter; DOC, dissolved organic carbon; DON, dissolved organic nitrogen.

Sources: 1, Fahey et al. 2005 (Table 1); 2, Dittman et al. 2007 (Table 1); 3, Vandenbuwane et al. 2007 (Fig. 1); 4, Whittaker et al. 1979 (Table 3); 5, Fahey et al. 1988 (Table 3); 6, Acker 2006 (pp. 31, 55); 7, Mikolajkow 2003 (Fig. 3); 8, Yanai 1992 (Table 3).

CALIBRATION

Steady state.—The calibration and all simulations are based on the year 2000 daily total shortwave irradiance, maximum and minimum daily temperature, and precipitation records from Hubbard Brook (Bailey et al. 2003). We assume a constant 360 μmol/mol CO$_2$ concentration throughout the simulations, and distribute the NH$_4^+$, NO$_3^-$, PO$_4^{3-}$, and DON inputs evenly throughout the year (Tables 1 and 2). We calibrate the MEL model to match the carbon budget compiled by Fahey et al. (2005) for Hubbard Brook, New Hampshire under the assumption that this budget represents a steady-state condition for the forest (calibration details given in Tables 1 and 2 and Appendix: Table A1). For the N and P stocks and fluxes, we mainly use data reported in Whittaker et al. (1979) and Yanai (1992; other sources are listed in Tables 1 and 2). However, because of year-to-year differences in nutrient budgets and differences in methodologies, where appropriate we adjust N and P numbers to be consistent with the Fahey et al. (2005) C budget by dividing the Fahey et al. C numbers by the C:N and C:P ratios reported in other data sources (see

source and notes columns in Tables 1 and 2). Physical and physiological parameters are based on literature values, and we use values for northern hardwood forests where possible (see Appendix: Table A2 for sources). Major rate parameters for the flux equations are calibrated to match the annual cumulative flux rates (see Table 2).

Woody-litter production in early succession.—Although most of the model parameters can be constrained by the steady-state calibration, the relative turnover rate of woody biomass changes during succession and therefore needs additional data to be constrained (compare solid and dashed lines in Fig. 2). These successional changes in relative turnover reflect competitive interactions among trees as the forest undergoes canopy closure and self-thinning, and are therefore difficult to represent explicitly in an aggregated biogeochemical model like the MEL model. Our implicit representation of these processes is to increase coarse-woody turnover during the canopy closure phase of succession (Fig. 2; Eq. A.73). Data on woody turnover are not directly available; we therefore calibrate the

turnover parameters based on the accumulated above-ground biomass for forests of different ages in the White Mountain region of New Hampshire, USA (S. P. Hamburg, *unpublished data*; Fig. 2). We base the calibration on recovery from a bole-only harvest, as we will describe for the base simulation.

Initial conditions.—All of our simulations are of succession following a disturbance in which only a fraction of the steady-state live biomass remained and varying amounts of dead biomass are left on site (Table 3). To adjust the allocation of uptake effort among resources to reflect the requirements of the young forest, we allow the efforts (V_i) to adjust to the initial conditions by iterating the first year of the simulation until $\Omega_i = 1/\Phi$ for all i (Eq. 1). The simulations begin from this condition of balanced resource acquisition.

ANALYSES AND RESULTS

We ran nine sets of 200-year simulations with the MEL model. The principal results from each of these simulations will be presented, together with analysis and interpretation of the results.

Base simulation.—For the base simulation, we simulate a bole-only, clear-cut harvest in which 19% of the plant C, 9% of the plant N, and 5% of the plant P is removed from the ecosystem (amounts based on Watershed 4 at Hubbard Brook; Yanai 1998), 1% of the biomass is left alive to initialize regrowth, and the remaining 80% of plant biomass is left on site as dead organic matter (Table 3). We set the N and P in initial biomass based on the vegetation allometry and pre-scribed tissue nutrient concentrations (q_{LN}, q_{WN}, q_{RN}, q_{LP}, q_{WP}, and q_{RP} in Appendix: Eqs. A.43–A.44; see *Allometry* section in Appendix: Table A2). All of the material removed in the harvest is woody (nonactive) biomass. All of the leaves and fine roots and 5% of the preharvest woody biomass (including 5% of woody roots) are added to the Phase I material. We add the remaining woody biomass to the coarse woody debris.

Nutrients fueling recovery of plant biomass following a bole-only harvest are derived predominantly from sources inside the ecosystem (Fig. 3b, c). Immediately after the harvest (years 0–5), mineralization remains high but plant demand is low, so soil nutrient concentrations are high and biomass accumulation is limited by photosynthetic capacity; the majority of the uptake effort is therefore allocated to photosynthesis (Fig. 4c). Within a few years (years 5–13), there is a transfer of N and P from Phase I SOM and coarse woody debris to plant biomass and Phase II SOM. In mid-to-late succession (years 13–100), most of the N and P supporting plant growth are derived from Phase II SOM (Fig. 3b, c). Entrainment of nutrients from outside the ecosystem is too slow to support observed rates of plant biomass recovery (solid circles in Fig. 2). The internal support for plant recovery is possible because (1) plants contain a relatively small fraction of the actively cycling nutrient capital in SOM and plants

($\sim$8.6% for N, 16.5% for P, vs. 41% for C) and (2) in a bole-only harvest, only the least nutrient-rich tissues are removed from the site. The result is that <1% of the actively cycling ecosystem N and P are removed in a bole-only harvest, compared to 7.7% of the C.

Despite this relatively small loss of nutrient capital in the harvest, the postharvest residues set up an imbalance in the N vs. P cycles. The N:P ratio of the postharvest plant residue is less than half the N:P ratio of the soil organic pools (Table 3; Whittaker et al. 1979, Yanai 1998); when added to the soil, this material decreases the N:P ratio of Phase I SOM by $\sim$40% (Table 3). Furthermore, there is a more than sevenfold increase in the amount of coarse woody debris, which is eventually converted to Phase I SOM; the woody debris also has a 40% lower N:P ratio than the preharvest Phase I SOM (Table 3). The result is that, compared to the preharvest soils, soil organic P is initially in excess relative to N.

During the first 13 years of the simulation, this imbalance in organic soil N vs. P causes a shift in resource use by soil microbes such that the Phase I SOM (which includes the microbial biomass) retains N more strongly ($\sim$20% loss) than P ($\sim$50% loss). Consequently, within six years, plant and microbial uptake decrease the NH_4^+ and NO_3^- concentrations below the levels used for the steady-state calibration, but PO_4^{3-} is mineralized in excess of plant needs and its concentration in soil solution remains high (Fig. 4b). During this phase, uptake effort by plants is allocated away from photo-synthesis toward NH_4^+ and NO_3^- uptake; allocation toward PO_4^{3-} uptake remains low (Fig. 4c). Also during this time period, the nutrients fueling biomass regrowth are derived from the postharvest residue left in coarse woody debris and Phase I SOM; the high C:N ratio of material transferred from coarse woody debris to Phase I SOM stimulates immobilization of N, which results in only a 20% net loss of Phase I N compared to a 50% loss of C, but the low N:P ratio of the postharvest residue results in Phase I losses of P that are proportionally slightly higher than the C losses (Fig. 3a, c). Phase II SOM also accumulates C, N, and P during this period. However, nutrients mineralized from coarse woody debris and Phase I SOM are only partially offset by nutrient accumulation in biomass and in Phase II SOM (Fig. 3b, c), resulting in a net loss of C, N, and P from the ecosystem (Fig. 4a). During the first 13 years, leaching and the formation of secondary P minerals results in a loss of 4% of the actively cycling ecosystem P capital in addition to the 1% removed in the harvest; the ecosystem N capital decreases by <1% during the same period.

After about year 13 of the simulation, Phase II SOM begins to lose C, N, and P and Phase I SOM begins to accumulate N but not P (Fig. 3b, c). P availability remains high relative to N and plant N uptake effort remains high relative to P uptake effort (Fig. 4c). Thus, between years 13 and 25, $\sim$75% of the N fueling biomass

TABLE 2. Multiple element limitation (MEL) model state variables and fluxes; flux values are given as annual totals but have per-day units in the model.

Variable or flux	Term	Value	Notes and sources
Effort (fraction of total)			partitioned between canopy and roots based on leaf and root biomass (Appendix: Eqs. A.82–A.83)
CO_2	V_C	0.218	assumes $V_C = V_I$ and root effort distributed evenly among N, P, and water
Light	V_I	0.218	
NH_4^+	V_{NH4}	0.155	partitioning between NH_4^+ and NO_3^- based on relative marginal yields
NO_3^-	V_{NO3}	0.033	
PO_4^{3-}	V_{PO4}	0.188	
H_2O	V_W	0.188	
Water (mm)			
Soil water	W	71	after model run of several years
Snowpack	W_{snow}	84	after model run of several years
Carbon fluxes (g C·m^{-2}·yr^{-1})			
Photosynthesis	U_C	1230	Fahey et al. (2005: Table 2)
Plant maintenance respiration	R_m	498	steady state for B_C
Plant growth respiration	R_g	158	28% of NPP; Waring and Schlesinger (1985: Table 2.3)
NO_3^- uptake respiration	R_u	11	$U_{NO3} \times NO_3^-$ uptake and assimilation cost from Appendix Table A2
Total plant respiration		667	sum of components
Net primary production		563	NPP of components; Fahey et al. (2005: Table 2)
Coarse woody litter	L_{CWC}	131	steady state for D_{Cc}
Fine litter	L_C	432	$NPP - L_{CWC}$
D_{Cc} to D_{C1} transition	T_{CWC}	131	10-yr residence time; Alban and Pastor (1993); Mattson et al. (1987)
Phase I respiration	R_{Cm1}	443	Steady state for D_{C1}
D_{C1} to D_{C2} transition	T_{DC12}	113	20% of litter inputs converted to Phase II material; Melillo et al. (1989)
Phase II respiration	R_{Cm2}	113	steady state for D_{C2}
DOC production	P_{DOM}	450	steady state for E_{DOM}
DOC uptake	U_{DOMm}	443	assumed equal to Phase I respiration; Schimel and Weintraub (2003: Fig. 4)
DOC inputs	I_{DOM}	2.03	$(I_{NH4} + I_{NO3}) \times$ DOC:inorganic N ratio from Currie et al. (1996:479)
DOC leaching	L_{DOM}	9.76	DON leaching × DOM C:N ratio from Appendix Table A2
Nitrogen fluxes (g N·m^{-2}·yr^{-1})			
NH_4^+ deposition	I_{NH4}	0.255	Buso et al. (2000: Table 8)
NO_3^- deposition	I_{NO3}	0.690	Buso et al. (2000: Table 8) + 0.14 g N/m^2 dry deposition; Lovett et al. (1997: Table 1)
DON deposition		0.076	I_{DOM}/DOM C:N ratio from Appendix Table A2
NH_4^+ leaching	L_{NH4}	0.003	steady state for total N budget × fraction NH_4^+ runoff from Currie et al. (1996: Table 7), hardwood deep-rooting zone
NO_3^- leaching	L_{NO3}	0.002	steady state for total N budget × fraction NO_3^- runoff from Currie et al. (1996: Table 7), hardwood deep-rooting zone
DON leaching		0.365	steady state for total N budget × fraction DON runoff from Currie et al. (1996: Table 7), hardwood deep-rooting zone
Nitrification	T_{Ntr}	7.768	55–60% of net mineralization; Groffman et al. (2001: Table 1)
Denitrification	T_{DNtr}	0.650	Groffman et al. (2001: Table 2)
Plant NH_4^+ uptake	U_{NH4}	11.055	steady state for E_{NH4}
Plant NO_3^- uptake	U_{NO3}	2.455	steady state for E_{NO3}
Coarse woody litter	L_{CWN}	0.580	L_{CWC}/C:N of coarse woody debris from Appendix Table A2
Fine litter	L_N	12.93	Fahey et al. (2005: Table 2) C litter cl'1asses/Whittaker et al. (1979: Table 5) C:N of litter OR × Fahey et al. (1988: Table 3) root %N/(C:DM)†
D_{Nc} to D_{N1} transition	T_{CWN}	0.580	steady state for D_{Nc}
Microbial NH_4^+ uptake	U_{NH4m}	48.688	4× plant N uptake (Nadelhoffer et al. 1999: Fig. 1); 90% of microbial uptake is NH_4^+ (Booth et al. 2005: Table 3)
Microbial NO_3^- uptake	U_{NO3m}	5.351	4× plant N uptake (Nadelhoffer et al. 1999 Fig. 1); 10% of microbial uptake is NO_3^- (Booth et al. 2005: Table 3)
Phase I N mineralization	R_{Nm1}	60.874	steady state for D_{N1}
D_{N1} to D_{N2} transition	T_{DN12}	6.385	T_{DC12}/C:N Phase II OM from Appendix Table A2
Phase II N mineralization	R_{Nm2}	6.385	steady state for D_{N2}
DON production		16.836	P_{DOM}/C:N of DOM from Appendix Table A2
DON uptake		16.547	U_{DOMm}/C:N of DOM from Appendix Table A2
Phosphorus fluxes (g P·m^{-2}·yr^{-1})			
PO_4^{3-} deposition	I_{PO4}	0.004	Yanai (1992: Table 3)
PO_4^{3-} leaching	L_{PO4}	0.002	Yanai (1992: Table 3)

TABLE 2. Continued.

Variable or flux	Term	Value	Notes and sources
°1 mineral weathering	T_{PAw}	0.0035	Crews et al. (1995 Fig. 3); 20 000 yr for Ca phosphates to disappear
°2 mineral weathering	T_{P2w}	0.002	assumes similar turnover rate as °1 minerals
°2 mineral formation	T_{PO4s}	0.0074	steady state for E_{PO4}
Plant PO_4^{3-} uptake	U_{PO4}	0.962	Yanai (1992: Table 3)
Coarse woody litter	L_{CWP}	0.0509	L_{CWC}/C:P of coarse woody debris from Appendix Table A2
Fine litter	L_P	0.911	steady state for B_P
D_{Pc} to D_{P1} transition	T_{CWP}	0.051	steady state for D_{Pc}
Microbial PO_4^{3-} uptake	U_{PO4m}	7.72	assume a 7:1 N:P mass ratio for microbial uptake; Redfield (1958)
Phase I P mineralization	R_{Pm1}	8.26	steady state for D_{P1}
D_{P1} to D_{P2} transition	T_{DP12}	0.422	T_{DC12}/C:P Phase II OM from Appendix Table A2
D_{P2} mineralization	R_{Pm2}	0.422	steady state for D_{P2}
Water fluxes (mm/yr)			
Precipitation	I_{ppt}	1451	Bailey et al. (2003)
Interception	I_{nt}	212	$P_{pt} - (I_{rain} + I_{snow})$; assumed to evaporate
Rainfall	I_{rain}	⋯	calculated internally (Appendix Table A1, Eq. A.134)
Snowfall	I_{snow}	⋯	calculated internally (Appendix Table A1, Eq. A.135)
Throughfall and stem flow	$I_{rain} + I_{snow}$	1239	equations from Leonard (1961)
Snowmelt	T_{SM}	⋯	calculated internally (Appendix Table A1, Eq. A.137)
Runoff	R_O	941	Bailey et al. (2003)
Transpiration/water uptake	U_W	297	$I_{rain} + I_{snow} - R_O$
Evapotranspiration		510	$I_{nt} + U_W$

† For roots, litter N was calculated as $L_N = L_C \times p_r/c$, where L_C is the root litter C from Fahey et al. (2005), p_r is the percentage of N in roots from Fahey (1988), and c is the C to dry mass ratio (0.45) used in the model. For other tissues, litter N was calculated as $L_N = L_C/q$, where q is the C:N ratio of the litter class from Whittaker et al. (1979).

regrowth is derived from Phase II SOM and the remainder from coarse woody debris. The P released from coarse woody debris, Phase I SOM, and Phase II SOM is more than is needed for the biomass regrowth, so the PO_4^{3-} concentration remains high, and the ecosystem loses another 4% of the actively cycling P capital (Fig. 4a).

By year 25 of the simulation, the recovering ecosystem shifts from a state where the P needed for regrowth is in excess supply relative to N to a state where N is in excess relative to P. During this transition when N limitation is eased, but P limitation has not fully established, plant uptake effort is reallocated toward photosynthesis (Fig. 4c). This transition happens because N and P from the postharvest residue have been exhausted, Phase I SOM begins to immobilize P in addition to N, and all of the nutrients fueling biomass regrowth are derived from Phase II SOM (Fig. 3). The N:P ratio of Phase II SOM is about twice the N:P of the regrowing vegetation and, as a result, PO_4^{3-} concentrations drop, NH_4^+ and NO_3^- concentrations increase (Fig. 4b), losses of P capital from the ecosystem stop, and losses of N capital increase, although only slightly (Fig. 4a). By the end of this transition, plant uptake effort has been reallocated from N to P (Fig. 4c).

The increased woody litter production associated with canopy closure promotes soil P loss relative to N via the same mechanisms that regulated the processing of the initial harvest residues, although the effects are more subtle. Woody litter production peaks in about year 30 of the simulation (Fig. 2), but its effect on soil processes lags by several years because of the residence time in

coarse woody debris. As with the postharvest residue, this woody litter has a lower N:P ratio than the SOM. As a consequence, N is immobilized into Phase I SOM (Fig. 3b), NH_4^+ and NO_3^- concentrations decline (Fig. 4b), and PO_4^{3-} concentrations increase slightly between years 35 and 80 of the simulation (this decline in N and increase in P does not occur in the simulation, depicted by the dashed line in Fig. 2, with constant woody litterfall rates and no woody litter pulse at canopy closure). In response to the changes in nutrient concentrations, plant uptake effort is reallocated from P back to N (Fig. 4c). Throughout this period, the nutrients fueling biomass regrowth are derived predominantly from Phase II SOM, and by year 80 the biomass has reached ~90% of its steady-state value.

After year 80, the effects of the woody litter produced during canopy closure have dissipated, Phase I SOM begins to mineralize N, and NH_4^+ and NO_3^- concentrations again increase and uptake effort is allocated back toward P (Fig. 4b, c). Between years 80 and 130, leaching and denitrification drive a 4% loss of ecosystem N, which brings the ecosystem N and P cycles back into near synchrony, with the amounts of both ~8% below the stocks in the calibrated steady state (Fig. 4a). During this period, biomass accumulates C and P but loses N; coarse woody debris remains nearly constant; Phase I SOM accumulates C but loses a small amount of P and a large amount of N; and C, N, and P in Phase II SOM decline until year 110, and then begin to accumulate.

By year 200, the major ecosystem C, N, and P stocks have begun to level off at a value between 6% and 12% below the steady-state values used in the calibration and

the distribution of uptake effort is nearly equal for N and P, as it is in the mature forest (Fig. 4c). The total C, N, and P stocks in the ecosystem are all ~8% below the steady state (Fig. 4a).

This 8% net C loss from the ecosystem is about equivalent to the amount of C fixed in photosynthesis in two years and could be recovered quickly. However, recovering the nutrients lost following the harvest is more difficult. The net loss of N is equivalent to 75 years of background N inputs and would take at least that long to recover. Recovering the P would take over 700 years even if there were no net production of secondary minerals, no leaching losses, and the supply from weathering of primary minerals remained constant. As a result, the re-accumulation of ecosystem C, N, and P and the resynchronization of the N and P cycles are constrained predominantly by the accumulation of P.

Constant distribution of uptake effort.—To assess the importance of optimizing uptake effort, we reexamine the bole-only simulation with the distribution of uptake effort held constant at the initial, steady state, and year 15, 30, 40, 65, 75, and 100 distributions; we select these years based on the peaks in effort for C, N, and P resources in the base simulation (Fig. 4c). Biomass recovery is sensitive to the reallocation of uptake effort as soil and canopy conditions change during recovery. Thus, only with the initial distribution of effort does the vegetation survive for more than 20 years (Fig. 5). With effort held constant at the initial distribution, the vegetation accumulates ~2.9 kg C/m² in 40 years, but accumulates no further biomass thereafter because the plants are limited by their nutrient uptake potential.

Post-disturbance organic residue.—To assess the importance of the initial nutrient removal, we simulate ecosystem recovery from a whole-tree harvest and a hurricane blowdown (Table 3). In the whole-tree harvest, we remove most of the aboveground biomass and leave less postharvest residue on site (based on Watershed 5 at Hubbard Brook; Yanai 1998). In the hurricane blowdown, we leave 99% of the biomass on site as residue. In both simulations, we again leave 1% of the biomass alive to initialize regrowth.

The residue left following the bole-only harvest clearly has important ramifications on the regrowth of vegetation in our base simulation; it is this residue that provides the nutrients to support the early stages of vegetation recovery and it is the N:P chemistry of this residue that sets the initial imbalance between N and P in the soil and desynchronizes the N and P cycles. Rerunning the simulation with a whole-tree harvest (less residue remaining) and with a hurricane blowdown (more residue remaining) results in dynamics qualitatively similar to those in the bole-only simulation (Fig. 5), including the general patterns of nutrient retention and loss. Despite the different tissues left in the residue, the initial N:P ratios of SOM in these simulations are close to those in the base simulation. The major difference is in the initial amount of coarse woody
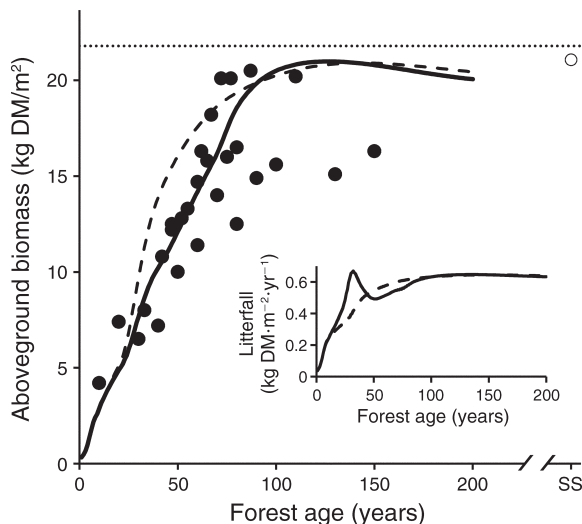

Fig. 2. Simulated and observed aboveground biomass in New England forests. Solid circles are unpublished data assembled by S. P. Hamburg and his students for the White Mountains of New Hampshire representing repeated observations of a series of sites with differing disturbance histories. The horizontal dotted line is the regional average for mature forests. The open circle indicates the mature-stand data from Fahey et al. (2005) to which the MEL model is calibrated. Solid and dashed black lines are our simulations of recovery following a bole-only harvest using the MEL model. In the simulation for the dashed line, we assumed that the relative turnover of woody biomass is constant at the rate calibrated for the steady state, SS (Appendix: Eq. A.73, $m_{CWX} = 0$; root mean square error (RMSE) = 3.8 kg DM/m²; root mean relative error (RE) = 26%). In the simulation for the solid line, we increased the turnover of woody biomass during canopy closure to account for species replacement and stand self-thinning ($m_{CWX} = 1.5 \times 10^{-4}$; RMSE = 2.7 kg DM/m²; RE = 20%). The inset shows the total litterfall rate for both simulations. For both simulations, we assumed that the aboveground–belowground biomass distribution (79%–21%) reported in Fahey et al. (2005) for a mature forest applies throughout recovery and that dry mass is 45% C.

debris (Table 3). The rates and magnitudes of vegetation regrowth would be indistinguishable among the three simulations, given natural variability (e.g., site fertility, species composition) among real-world sites and sampling error (compare Figs. 2 and 5). Nevertheless, there are quantitative differences among the three simulations that are enlightening.

First, even though there is less N and P left on site in the whole-tree harvest than there is in the bole-only harvest, there are larger nutrient losses immediately after the whole-tree harvest because there is less postharvest residue to immobilize and retain nutrients. The lack of residue to drive microbial growth also means that competition for nutrients by soil microbes is weaker and plants can initially accumulate more biomass following a whole-tree harvest than following a bole-only harvest (Fig. 5). Conversely, even though more N and P are left on site following a hurricane than a harvest, post-hurricane nutrient losses are less than the

TABLE 3. Initial C, N, and P distributions in simulations of recovery from a bole-only harvest, a whole-tree harvest, and a hurricane blowdown, along with the corresponding values for the mature stand.

Distribution	Mature stand	Bole-only harvest	Whole-tree harvest	Post hurricane
Carbon (g C/m²)				
Plants	12 006	120	120	120
Coarse woody debris	1 313	10 030	3 451	12 280
Phase I SOM	2 970	3 889	3 493	3 889
Phase II SOM	12 770	12 770	12 770	12 770
Removed in harvest	0	225	9 225	0
Total	29 059	29 059	29 059	29 059
Nitrogen (g N/m²)				
Plants	80.64	2.71	2.71	2.71
Coarse woody debris	5.80	44.31	15.24	54.24
Phase I SOM	130.72	162.74	154.71	160.20
Phase II SOM	724.18	724.18	724.18	724.18
Removed in harvest	0.00	7.40	44.50	0.00
Total	941.34	941.34	941.34	941.34
Phosphorus (g P/m²)				
Plants	10.94	0.27	0.27	0.27
Coarse woody debris	0.51	3.89	1.34	4.76
Phase I SOM	6.83	13.52	11.67	13.25
Phase II SOM	47.89	47.89	47.89	47.89
Removed in harvest	0.00	0.60	5.00	0.00
Total	66.17	66.17	66.17	66.17

Notes: All values are for 1 January of the first year of the simulations. Sources for the mature stand are given in Table 1. Data for biomass removed in harvest are from Yanai (1998).

postharvest losses because of the large amount of C-rich residue that promotes immobilization and retention of nutrients. Consequently, competition for nutrients by soil microbes is stronger after the hurricane than after either harvest, so that biomass initially accumulates more slowly following the hurricane (Fig. 5).

Second, removal of more N and P in the whole-tree harvest increases the effect of nutrient immobilization associated with woody litter production during canopy closure. The production of woody litter during canopy closure is roughly equivalent in all three simulations. However, because there is less N and P left in the ecosystem after the whole-tree harvest, the decline in growth rate associated with the increase in nutrient immobilization following the pulse of woody litter deposition is much stronger in the whole-tree harvest simulation than in the other two simulations (Fig. 5; years 30–50). Therefore, in the recovery following a whole-tree harvest, plant growth decreases sharply between years 30 and 50 and biomass accumulation in the other two simulations overtakes biomass accumulation in the simulation of recovery from a whole-tree harvest (Fig. 5).

Finally, biomass at the end of the simulations reflects the retained nutrient capital in the three simulations (Fig. 5). Following the whole-tree harvest, which has the highest nutrient removal and largest postharvest nutrient loss, biomass in year 200 is 5% lower than in the bole-only simulation; P is also 5% lower, although N is only 1% lower, indicating the persistent effects of P loss early in succession. Following a hurricane blowdown,

which has no initial nutrient removal and the smallest post-disturbance nutrient loss, biomass in year 200 is 1.8% higher than in the bole-only simulation; N and P are, respectively, 1.6% and 1.3% higher.

Buffered NH_4^+ and PO_4^{3-}.—In the base simulation, high PO_4^{3-} concentrations result in a loss of 8% of the ecosystem P in the first 25 years of the simulation. During that same period, NH_4^+ and NO_3^- concentrations are depleted by plant uptake and limit biomass recovery. To assess the importance of these changes in nutrient concentration on ecosystem recovery, we buffer the NH_4^+ and PO_4^{3-} concentrations in soil solution. To impose this buffering, we increase the amount of NH_4^+ or PO_4^{3-} by an order of magnitude in the steady-state calibration (to 8 g NH_4^+-N/m² and 0.81 g PO_4^{3-}-P/m²) and adjust the affinity parameter in the Langmuir isotherm (ε_{NH4} and ε_{PO4} in Appendix Eqs. A.23 and A.26) to compensate so that the soil solution concentrations in the mature forest are unaffected and all of the NH_4^+ or PO_4^{3-} increase is in the fraction adsorbed to soil particles. We analyze buffering of each nutrient alone and of both nutrients in combination.

Buffering the soil solution NH_4^+ alone only has a small effect on the pattern of ecosystem recovery. Most importantly, buffering NH_4^+ lessens NH_4^+ depletion during the N-limited phase of succession (years 5–25), allowing plants to allocate more effort toward acquiring P, thereby retaining P in the ecosystem (Fig. 6c). This mechanism decreases the ecosystem P loss from 8% to 7% (plus the 1% loss in the harvest). Buffering NH_4^+ also decreases the spikes in NH_4^+ and NO_3^- concentra-
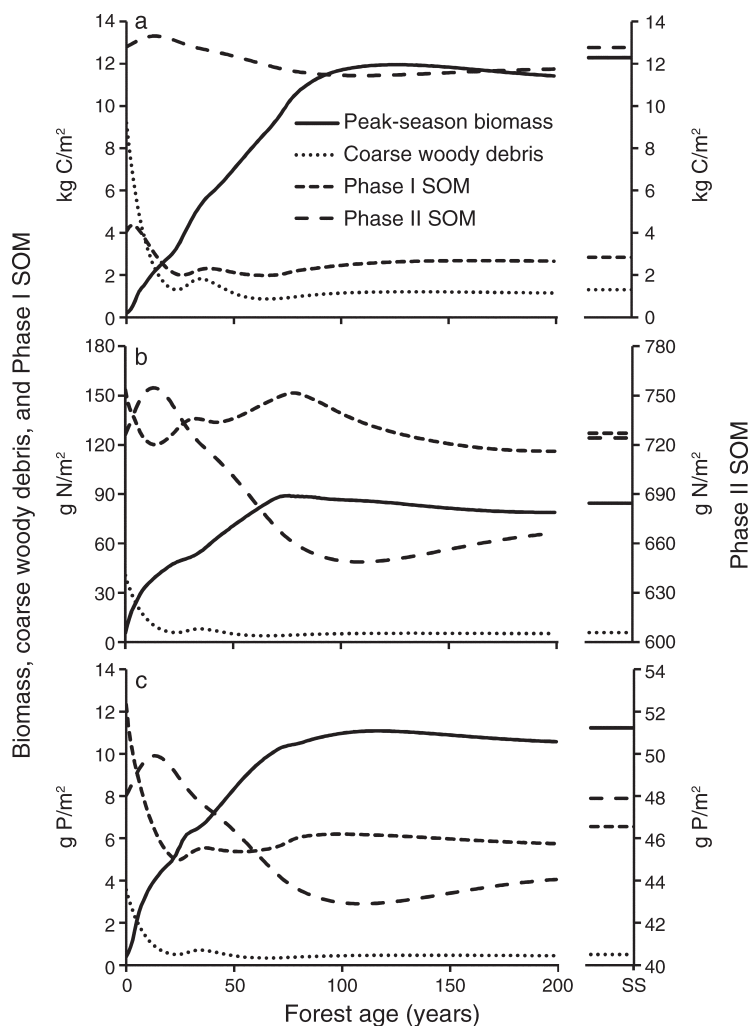
FIG. 3.   C, N, and P stocks in the major ecosystem components following a bole-only harvest. The steady-state (SS) values to which the MEL model is calibrated are graphed on the far right of each panel. Scale numbers for the Phase II SOM (long-dashed line) are on the right-hand axis.

tions in years 35 and 90 (Fig. 6e), which slows the N loss rate from the ecosystem. However, this slower loss only prolongs the time required to resynchronize the N and P cycles; because of the slow supply rate of P to the ecosystem and the stoichiometric constraints on the ecosystem components, the resynchronization in the model has to be realized through a loss of N rather than a gain of P.

Buffering the PO_4^{3-} concentration, both alone and in combination with NH_4^+, dramatically decreases the elevated PO_4^{3-} concentrations for 25 years following the harvest and reduces the associated P loss from 8% of the ecosystem P capital to only 3% (Fig. 6c). This reduction in early P loss results in less severe P limitation later in succession and therefore decreases the spikes in NH_4^+ and NO_3^- concentrations in years 35 and 90 (Fig. 6e). Higher P retention early in succession means less N needs to be lost to resynchronize the N and P cycles. The

ecosystem therefore retains both more P and more N when PO_4^{3-} concentration is buffered. Buffering NH_4^+ in addition to PO_4^{3-} has only a small additional effect on the C, N, or P cycles (Fig. 6).

Coarse woody debris turnover.—To assess the importance of the nutrient immobilization potential of coarse woody debris, we increase its turnover time from 10 to 20 years (halved r_{CW} in Appendix Eqs. A.97–A.99). This increase in turnover time also doubles the amount of coarse woody debris at steady state (doubles D_{Cc}, D_{Nc}, and D_{Pc}). Therefore, our initial conditions for this simulation have more coarse woody debris than in the base simulation, which amounted to an increase of 1313 g C/m², 5.8 g N/m², and 0.51 g P/m² in the ecosystem.

The major short-term effect of increasing the coarse woody litter turnover from 10 to 20 years is to slow the postharvest loss of C from the ecosystem (Fig. 6a). The slower supply of C-rich organic matter to microbes
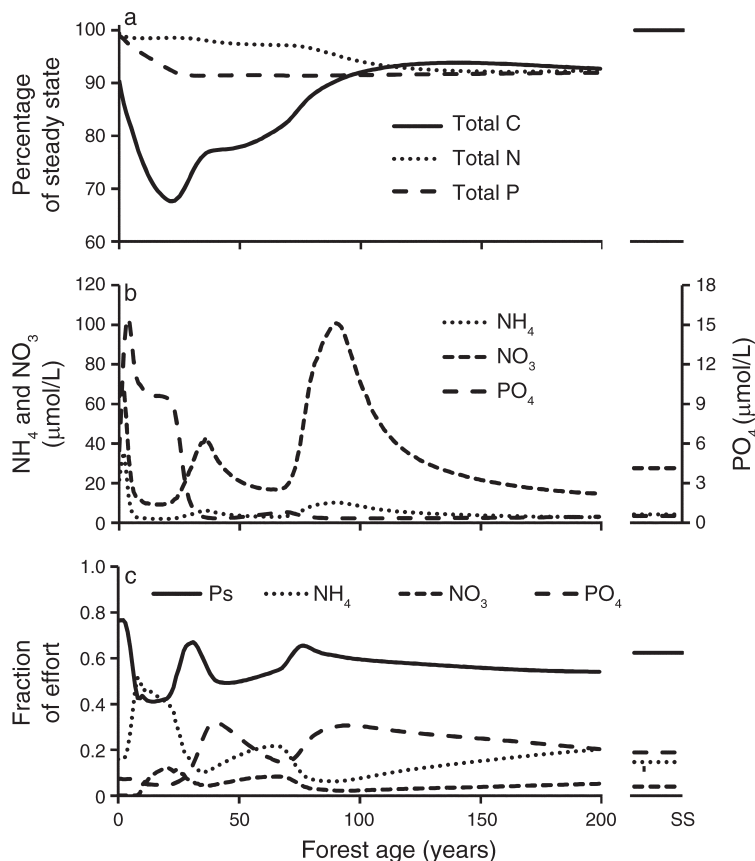
FIG. 4. Total ecosystem C, N, and P stocks (exclusive of primary and secondary minerals), soil solution NH_4^+ and NO_3^- (left-hand axis) and PO_4^{3-} (right-hand axis), and the allocation of effort by the plants toward acquiring resources following a bole-only harvest. The efforts allocated to CO_2, light, and water have been added together (photosynthesis, Ps) to simplify the figure. The steady-state (SS) values are graphed on the far right of each panel. Total C, N, and P are peak growing-season values (day 260 of the year, where day 1 is 1 January); nutrients and efforts are annual averages.

results in lower nutrient immobilization, higher nutrient concentrations in soil water (Fig. 6d–f), and therefore higher nutrient losses during the first 12 years. However, after about 12 years, the supply of C-rich substrate from the coarse woody debris serves to enhance immobilization, decrease nutrient concentrations in soil water (Fig. 6d–f), and retain nutrients in the ecosystem. Because the major loss of P is early in the recovery, this immobilization and retention is too late to stop most of the P loss. However, the enhanced immobilization associated with the larger amount of coarse woody debris and the prolonged supply of C-rich substrate to microbes does help retain N in the ecosystem. In addition, the slower turnover prolongs the period of N immobilization following canopy closure and self-thinning (Fig. 6d, e). The dynamics with a longer turnover time of coarse woody debris are therefore similar to the dynamics with a buffered concentration of NH_4^+, although the timing after year 30 is lagged and the later peaks in NH_4^+ and NO_3^- concentrations are about 20 years later in the

TABLE 4. Parameter values used in simulations with low and high gross : net mineralization ratios for N and P.

Parameter or variable	Base	Gross : net mineralization			
		Low N	High N	Low P	High P
α_{NH4} (g N·g^{-1} C·d^{-1})	1.68×10^{-4}	6.72×10^{-5}	4.20×10^{-4}	1.68×10^{-4}	1.68×10^{-4}
α_{PO4} (g P· g^{-1} C ·d^{-1})	2.10×10^{-5}	2.10×10^{-5}	2.10×10^{-5}	1.05×10^{-5}	4.20×10^{-5}
ψ_{Nm} (d^{-1})	1.16×10^{-4}	8.01×10^{-5}	1.50×10^{-4}	9.32×10^{-5}	1.33×10^{-4}
ψ_{Pm} (d^{-1})	5.27×10^{-4}	4.82×10^{-4}	5.69×10^{-4}	4.98×10^{-4}	5.48×10^{-4}
Gross : net N mineralization	8.98	4.67	19.76	8.98	8.98
Gross : net P mineralization	14.74	14.74	14.74	7.87	28.47

Note: Parameters are: α, microbial uptake rate constants (here, for NH_4 and PO_4); ψ, mineralization constant (here, for N and P); see Appendix: Table A2 for further details.

simulation with slower coarse woody debris turnover than with buffered NH_4^+.

Post-disturbance replanting.—The initial loss of nutrients, particularly P, in the base simulation is partly due to the low initial biomass and the associated low nutrient uptake potential of the vegetation. To assess the importance of this initial nutrient uptake potential, and to explore a potential mitigation strategy, we simulate recovery with 10% of the steady-state biomass remaining after the disturbance, but leaving the same amount of postharvest residue as in the base simulation; these initial conditions amount to planting additional vegetation equivalent to 9% of the initial biomass, which added about 4% to the total initial C in the ecosystem, 1.5% to the initial N, and 1.9% to the initial P.

The major effect of initializing the simulation with 10% of the steady-state biomass is to reduce the concentrations, and therefore the losses, of NH_4^+, NO_3^-, and PO_4^{3-} during the first eight years of the simulation. Because a substantial amount of the P loss is during the subsequent two decades, starting recovery with a higher biomass has little effect on the recovery after year 8. The total C, N, and P in the ecosystem therefore parallel the recovery in the base simulations, but are offset upward by the amount of C, N, and P added to the initial biomass plus the amount retained during the first eight years (Fig. 6).

Altered ratio of gross : net mineralization.—The dynamics of recovery in our simulations are strongly tied to the loss of nutrients, especially early in succession. An obvious way to curtail those losses in the simulations is to increase immobilization of nutrients into soil. We therefore altered the mineralization and immobilization parameters so that the net mineralization rates at steady state remain unchanged but the gross mineralization rates are either doubled or halved (Table 4). With a doubled gross : net mineralization ratio, there is also a higher immobilization rate and the microbes can compete better for nutrients against the vegetation; with a halved gross : net ratio, immobilization is slower and the microbes are poorer competitors with vegetation for nutrients.

The major effect of altering the gross : net mineralization ratio is to change the timing of the soil water NH_4^+ and NO_3^- peaks between years 50 and 150 (Fig. 7d, e) and the consequent loss of N from the ecosystem. With low gross : net mineralization ratios for either N or P, vegetation can compete better for nutrients, the vegetation recovers faster, and the peaks in NH_4^+ and NO_3^- concentration occur earlier and are smaller. The ecosystem therefore loses N earlier than in the base simulation, but, because of the faster recovery of vegetation, the ecosystem retains more N in the long term (Fig. 7b).

With high gross : net mineralization ratios for N, the microbes compete better for N during the N-limited phase of recovery between years 20 and 30, vegetation recovery is delayed, high PO_4^{3-} concentrations are
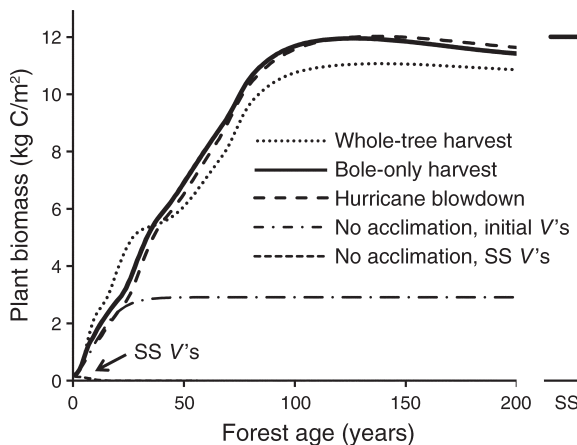

FIG. 5. Plant biomass recovery after a whole-tree harvest, a bole-only harvest, a hurricane blowdown, and a bole-only harvest but with no acclimation of uptake effort (initial and steady-state values for all the efforts, *V*s). In all simulations, biomass started at 1% of the calibrated steady state (SS, shown on far right of the graph). In the whole-tree harvest, 4.7% of the ecosystem N and 7.6% of the P is removed at the time of harvest. In the bole-only harvest, 0.8% of the ecosystem N and 0.9% of the P is removed. In the hurricane blowdown, all nutrients are left on site. Nutrients are also lost from the active ecosystem cycles through leaching, formation of secondary minerals, and denitrification. Two simulations with no acclimation are shown, one with the efforts frozen at their initial distribution in the bole-only simulation and the other with the efforts frozen at their distribution in the steady-state calibration.

prolonged (Fig. 7f), and more C and P are lost from the active ecosystem components than in the base simulation (Fig. 7a, c). Relative to the base simulation, the NH_4^+ and NO_3^- peaks between years 50 and 150 are delayed with high gross : net mineralization ratios for N because of the slower vegetation recovery and their height is lower because of the high immobilization (Fig. 7e); the result is a slight delay in N loss from the ecosystem but in the long term about as much N is lost as in the base simulation (Fig. 7b).

With high gross : net mineralization ratios for P, P immobilization is high and PO_4^{3-} concentration and ecosystem P loss are therefore lower early in recovery (Fig. 7c, f). This P retention results in higher N demand later in succession and the NH_4^+ and NO_3^- peaks between years 50 and 150 are lower, resulting in slower N losses later in succession (Fig. 7b).

Distribution of N and P between Phase I and Phase II SOM.—We examine the effects of redistributing the steady-state N and P between the younger, fast-turnover Phase I SOM and the older, slow-turnover Phase II SOM (Table 5). We assign high and low values for the Phase II C:N and C:P ratios (ϕ_N and ϕ_P in Appendix: Eqs. A.102–A.104, A.108–A.111), but keep the same total N and P in Phase I plus Phase II SOM as in the base simulation. We constrain our selection of Phase II SOM C:N and C:P ratios so that they are lower than those of Phase I SOM at steady state. We adjust Phase I
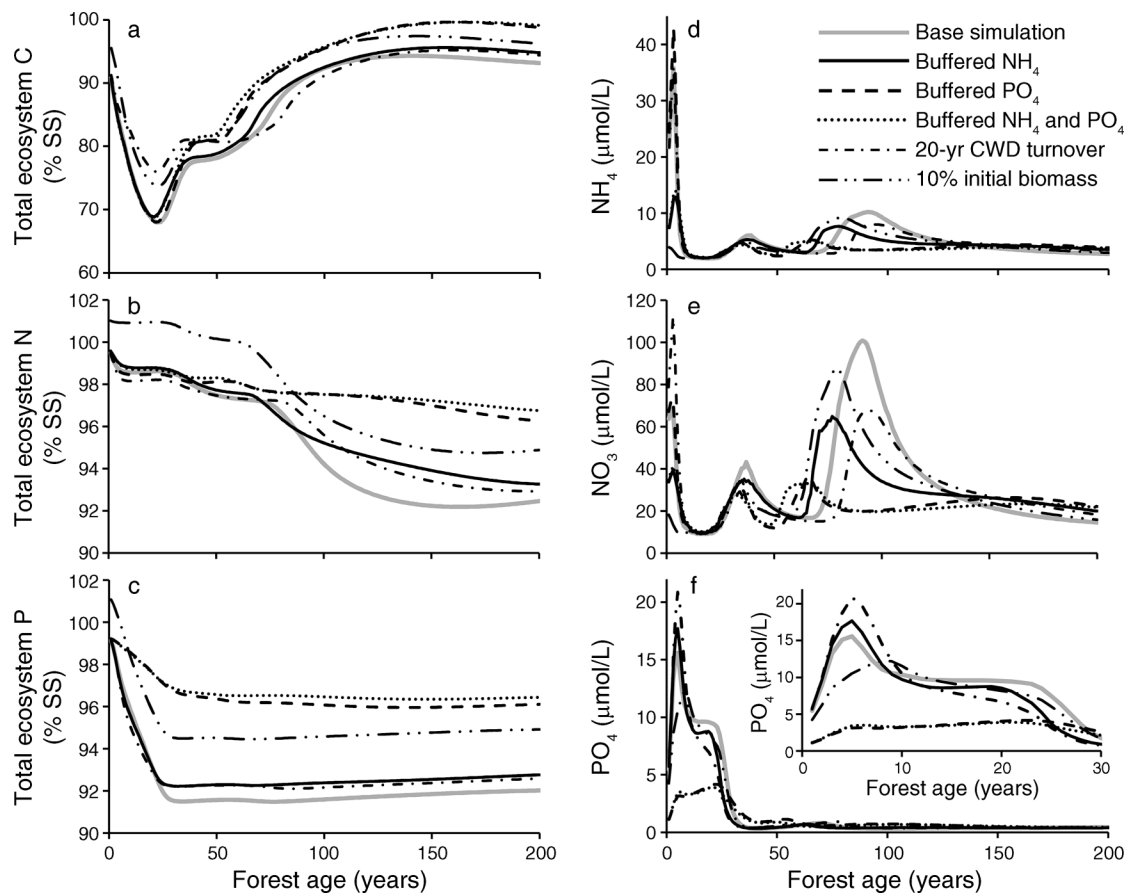
Fig. 6. Simulated recovery following a bole-only harvest when soil concentrations of NH_4^+ and PO_4^{3-} are buffered, when the turnover time of coarse woody debris (CWD) is increased from 10 to 20 years, and when the harvested site is planted with trees at 10% rather than 1% of the steady-state biomass. (a–c) Respectively, the peak-season (day 260 of the year) total ecosystem C, N, and P are plotted as a percentage of steady state (% SS). (d–f) Respectively, the annual average soil solution NH_4^+, NO_3^-, and PO_4^{3-} concentrations. The inset in panel (f) is a magnification of the first 30 years of the simulation.

and Phase II N and P values to be consistent with this change (D_{N1}, D_{N2}, D_{P1}, and D_{P2}). We then adjust the microbial NH_4^+, NO_3^-, and PO_4^{3-} uptake rate constants (α_{NH4}, α_{NO3}, and α_{PO4} in Appendix Eqs. A.102–A.104), the Phase I C, N, and P mineralization constants (ψ_m, ψ_{Nm}, and ψ_{Pm} in Appendix: Eqs. A.105–A.107), and the dissolved organic matter (DOM) production rate constant (r_{DOM} in Eq. A.115) so that microbial NH_4^+, NO_3^-, and PO_4^{3-} uptake, total soil respiration, total soil net and gross N and P mineralization, and DOM production are the same as in the base simulation.

Changes in the distribution of N and P between Phase I and Phase II SOM results in only small changes in the ecosystem C budget during recovery from harvest (Fig. 8a). Making Phase II SOM high in N ($\phi_N = 17$) results in higher NH_4^+ and NO_3^- peaks and faster ecosystem N losses between years 50 and 150, the time period when the Phase II SOM is still decreasing but N accumulation in vegetation has stopped (Fig. 3b). Low Phase II N ($\phi_N = 18.4$) results in lower peaks and slower losses.

However, redistribution of N between soil pools has little effect on N retention in the ecosystem by year 200.

Making Phase II SOM high in P ($\phi_P = 245$) means that the Phase I SOM at steady state is lower in P and hence the P immobilization needed to achieve this steady state is also lower. Consequently, P-rich Phase II SOM results in lower P immobilization immediately after the harvest and higher PO_4^{3-} concentrations and faster ecosystem P losses during the first eight years of the simulation (Fig. 8c, f). However, between years 8 and 30, the accumulation of Phase II SOM and the regrowth of vegetation decrease PO_4^{3-} concentrations and P losses from the ecosystem and the ecosystem is able to retain this P in the long term (Fig. 8c, f). Because of this long-term P retention, the peaks in NH_4^+ and NO_3^- and the associated N losses are lower between years 50 and 150 (Fig. 8d, e). With Phase II SOM low in P ($\phi_P = 285$), the opposite pattern of P and N losses and retention occurs, but the dynamics are less pronounced.

NH_4^+ and PO_4^{3-} fertilization.—In our interpretation of the results thus far, we infer alternating N- and P-
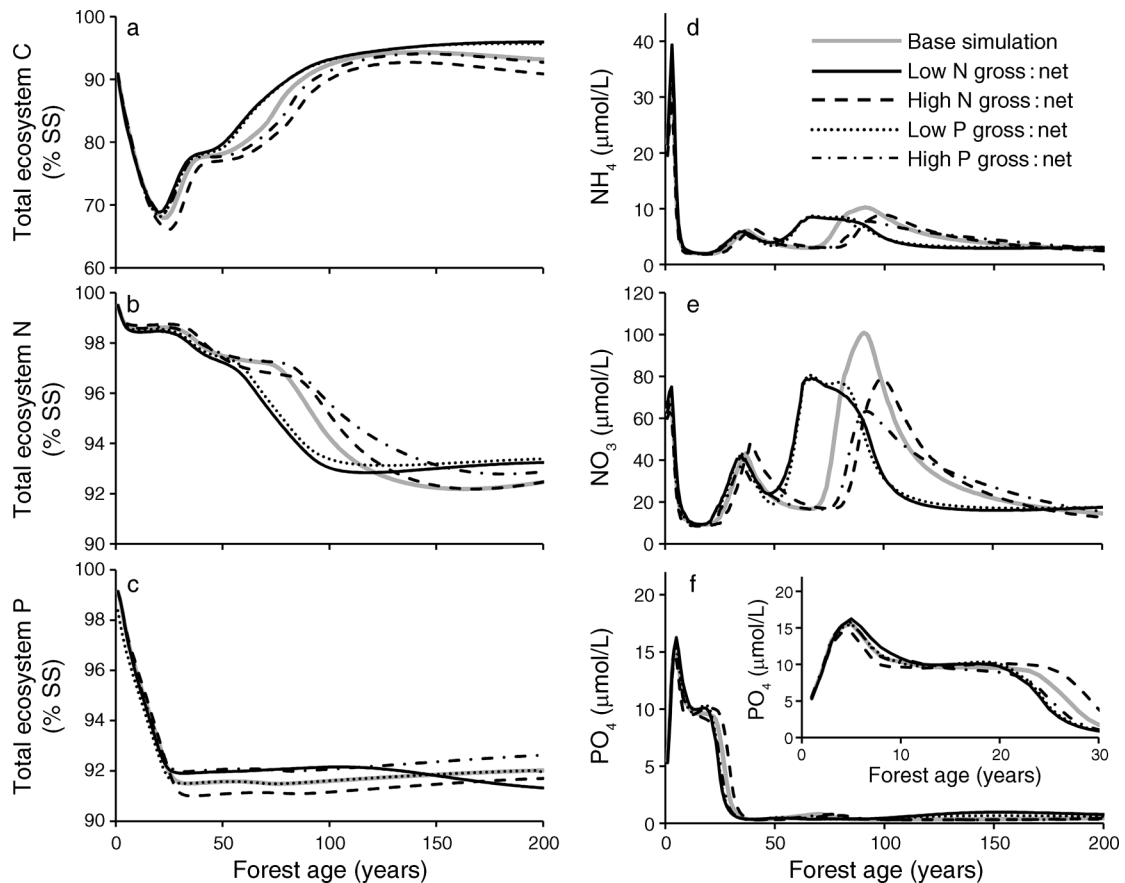
Fig. 7. Simulated recovery following a bole-only harvest with different gross : net mineralization ratios for N and P (Table 4). Panels are as described for Fig. 6.

limitation through most of succession with a final transition toward co-limitation at steady state. To corroborate this interpretation and to explore potential management options, we simulate fertilization with NH_4^+ and PO_4^{3-}, either individually or in combination, beginning in years 0, 15, 40, 65, or 100 of the base simulations and for the mature ecosystem at the calibrated steady state. These years correspond to periods of relative N vs. P limitation based on the distribution of plant uptake effort in the base simulation (Fig. 4c). We add 3 g $N \cdot m^{-2} \cdot yr^{-1}$ as NH_4^+ and/or 1 g $P \cdot m^{-2} \cdot yr^{-1}$ as PO_4^{3-} distributed uniformly between 15 May and 31 August.

For the fertilization beginning in year 0, there is only a weak biomass response (<6%) to any of the fertilizer additions during the first five years following the harvest, when all nutrient concentrations are elevated in the base simulation and biomass accumulation is limited by photosynthetic capacity (Fig. 9). Beginning in year 5, plant growth responds strongly to fertilization with NH_4^+. Because of this increase in plant growth, about half of the P that is lost in the base simulation is instead taken up by plants and retained within the ecosystem. The ecosystem does not respond to PO_4^{3-}

fertilization during this period and the biomass response to both NH_4^+ and PO_4^{3-} in combination is <2% higher than the response to NH_4^+ alone.

For the fertilization beginning in year 15, the ecosystem response is consistent with N limitation until about year 30, when it transitions to P limitation (Fig. 9a). Between years 15 and 30, plant growth increases in response to NH_4^+ and to NH_4^+ and PO_4^{3-} combined, but not to PO_4^{3-} alone. However, unlike the simulation with NH_4^+ fertilization beginning in year 0, the increased plant growth is too late in the simulation to significantly curtail the loss of P from the ecosystem. Nevertheless, the accelerated plant growth with NH_4^+ or NH_4^+ plus PO_4^{3-} fertilization results in earlier canopy closure and therefore an earlier pulse of coarse woody litter into the soil. The resulting increase in P immobilization causes the ecosystem to transition to P limitation earlier and causes plant growth to slow relative to the base simulation between years 25 and 35 (Fig. 9a). As a result, plant biomass in the base simulation overtakes the biomass in the simulations with NH_4^+ or NH_4^+ plus PO_4^{3-} fertilization during this period (Fig. 9a; similar to the dynamics in the whole-tree harvest in Fig. 5). After year 30, accumulated plant
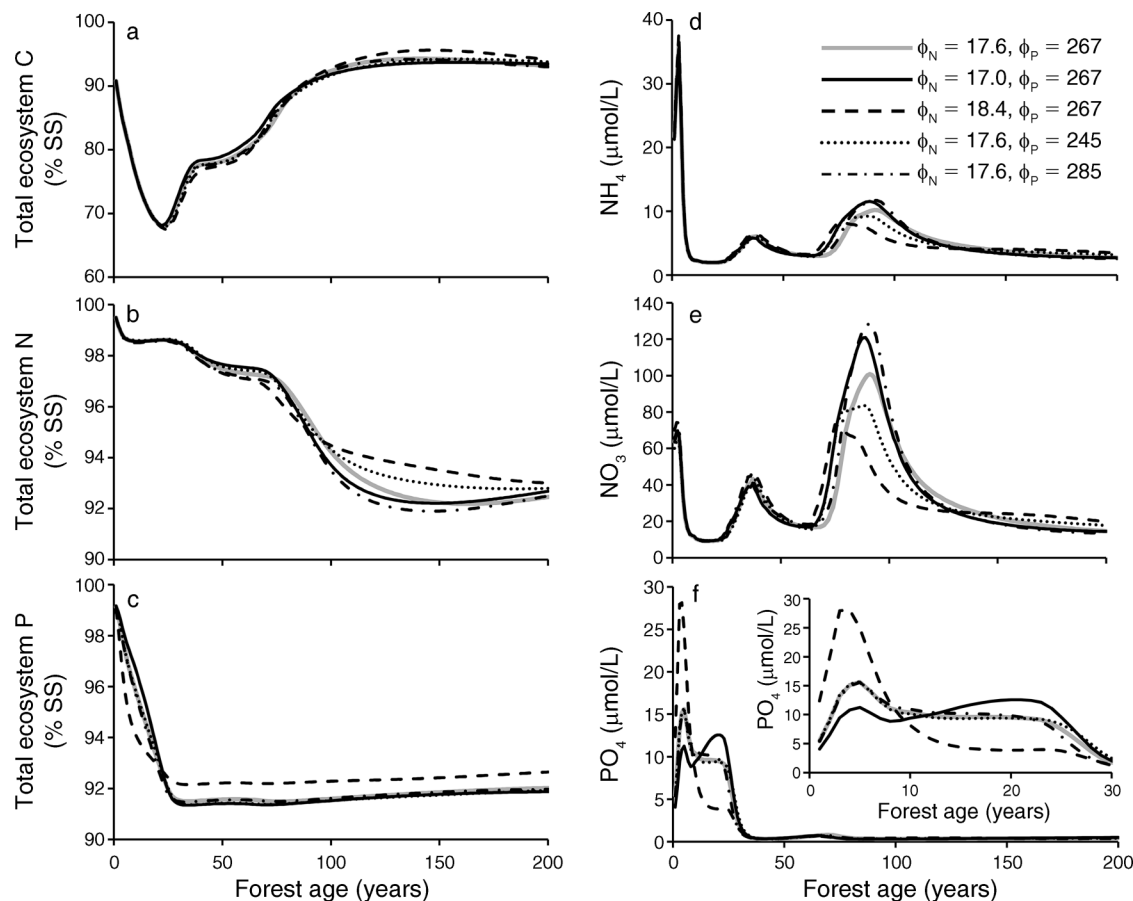
FIG. 8. Simulated recovery following a bole-only harvest with steady-state soil N and P redistributed between Phase I and Phase II soil organic matter (Table 5). Total soil C, N and P at steady state are kept constant among simulations. The C:N and C:P ratios of Phase II SOM are represented by ϕ_N and ϕ_P. Panels are as described for Fig. 6.

biomass is higher with PO_4^{3-} fertilization than with NH_4^+ fertilization (Fig. 9a). Because of the early canopy closure and associated nutrient immobilization in the simulation of fertilization with both nutrients, accumulated biomass is also higher with PO_4^{3-} fertilization alone than with both nutrients combined after about year 30.

In all the fertilizations beginning after year 40, plant growth remains P-limited (Fig. 9a). The response of plant growth to NH_4^+ fertilization becomes progressively weaker until there is virtually no response to NH_4^+ in the fertilization beginning in year 100. However, the synergistic effect of both nutrients in combination is strongest late in succession.

Starting at the calibrated steady state, when the N and P cycles are fully synchronized, vegetation growth increases in response to fertilization with either nutrient alone, but the response to fertilization with both nutrients in combination is stronger than the sum of the responses to fertilization with each nutrient alone.

The responses of the soil C, N, and P stocks to fertilization are mostly driven by the increase in litter inputs to the soil (see Plate 1). However, fertilization

also has a stimulatory effect on microbial activity in the model. The initial effect of fertilization is to increase C use efficiency by microbes (Appendix Eqs. A.105–A.114). However, in the long term (>10 years), fertilization lowers the C:N or C:P ratio of the soil, which decreases the microbial C use efficiency.

DISCUSSION

Most terrestrial ecosystems cycle N and P very tightly; annually the amount of N and P that enters the active ecosystem cycle from deposition or weathering of primary and secondary minerals is <10% of the N and P that cycles within the ecosystem. We propose that this tight cycling and the stoichiometric constraints on vegetation and soil microbes result in the synchronization of the N and P cycles such that the ratio of N:P in plant uptake, litterfall, and net mineralization are nearly equal at steady state (14.04 for our model; Table 2). We further hypothesize that this synchrony is disrupted by disturbance and that this disruption results in differential losses of N vs. P at different stages of recovery, but that the responses of vegetation and microbes drive the
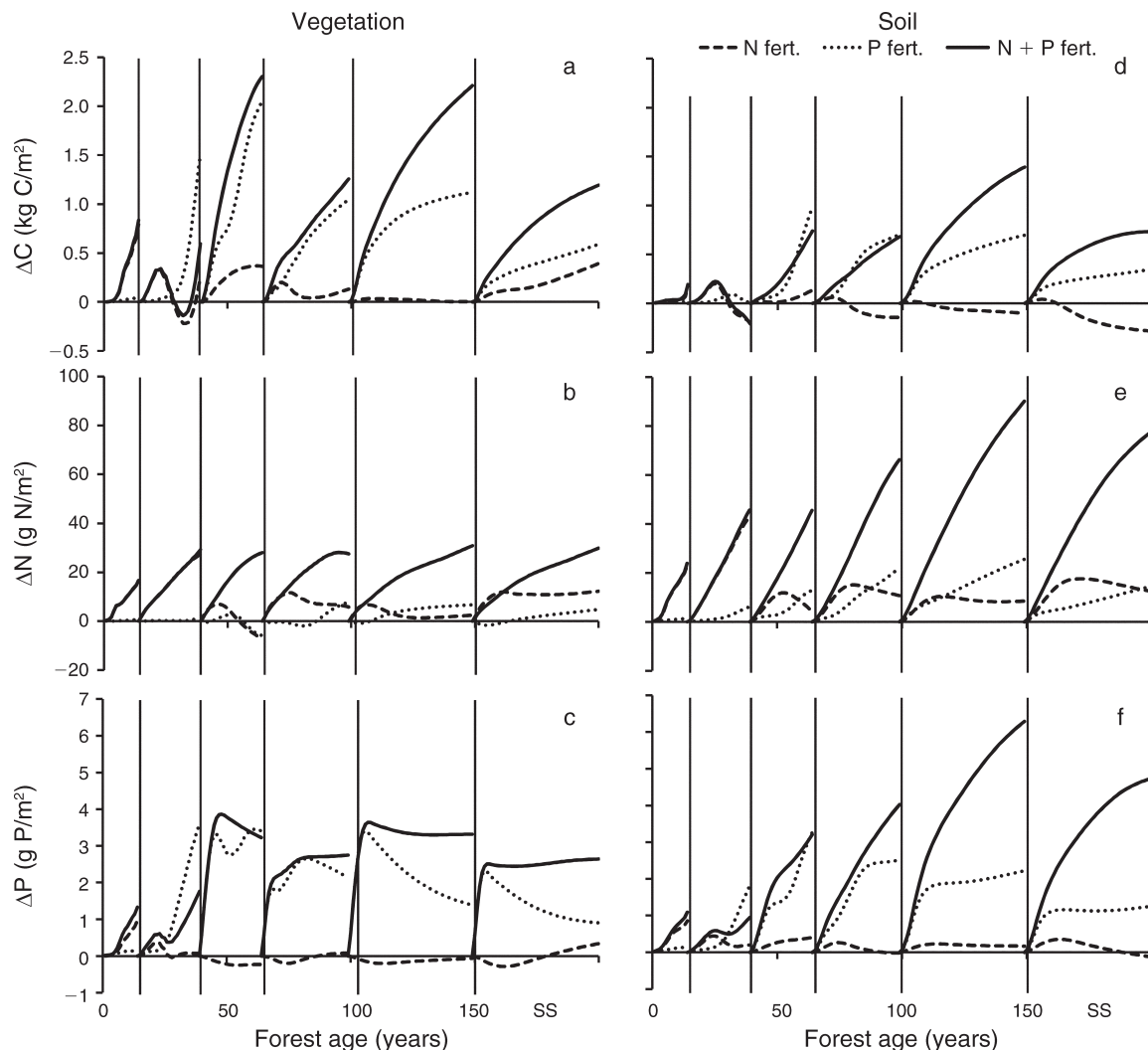
FIG. 9. Change in C, N, and P in (a–c) vegetation and (d–f) soils relative to the base simulation following N, P, and NP fertilizations (fert.) at years 0, 15, 40, 65, and 100 and at steady state (SS). Plotted values equal the values from the fertilization simulation minus the values from the base simulation.

ecosystem toward a resynchronization of the element cycles.

Removal of N and P in a bole-only harvest is a relatively small disruption to these cycles; a larger disruption is associated with the losses of nutrients immediately following the harvest when decomposition is faster than net primary production, soils lose organic matter (Bormann and Likens 1979, Houghton et al. 1983, Yanai et al. 2003), and mineralization remains high but plant nutrient demand is small (Marks and Bormann 1972, Covington and Aber 1980). During this phase, the vegetation is limited by its own photosynthetic capacity and most of the uptake effort in our model is allocated toward photosynthesis and away from N and P uptake (Fig. 4c). In our model, the vegetation cannot survive this initial period of recovery without this pronounced allocation toward photosynthesis. Without the subse-

quent reallocation of uptake effort to nutrients, the vegetation cannot recover fully (Fig. 5).

Following this initial period of N and P loss, our model predicts an additional loss of P associated with the low N:P ratio of the residue left after the harvest. This low N:P ratio results in a shift in microbial use of organic and inorganic resources such that there is a preferential retention of soil N and release of P and a consequent buildup of PO_4^{3-} in soil solution. Plant responses exacerbate this buildup by allocating uptake effort toward the more limiting resource (N) and away from the more abundant resource (P). As a result of this PO_4^{3-} buildup, 8% of the ecosystem P capital is lost from the active ecosystem cycle through leaching to deeper soil layers and formation of secondary minerals in the first 25 years after the harvest (Fig. 4a). This loss of P brings the N and P cycles closer to synchrony with the

TABLE 5. Parameter values and Phase I and Phase II soil C, N, and P values used in simulations with N and P redistributed between Phase I and Phase II soil pools.

Parameter	Base ϕ_N and ϕ_P	Low ϕ_N	High ϕ_N	Low ϕ_P	High ϕ_P
ϕ_N (g C/g N)	17.63	17	18.4	17.63	17.63
ϕ_P (g C/g P)	267	267	267	245	285
α_{NH4} (g N· g^{-1} C ·d^{-1})	1.68×10^{-4}	1.28×10^{-4}	2.16×10^{-4}	1.68×10^{-4}	1.68×10^{-4}
α_{NO3} (g N· g^{-1} C ·d^{-1})	2.35×10^{-5}	1.80×10^{-5}	3.02×10^{-5}	2.35×10^{-5}	2.35×10^{-5}
α_{PO4} (g P· g^{-1} C ·d^{-1})	2.10×10^{-5}	2.10×10^{-5}	2.10×10^{-5}	7.34×10^{-6}	3.26×10^{-5}
ψ_m (d^{-1})	2.18×10^{-4}	2.16×10^{-4}	2.21×10^{-4}	2.15×10^{-4}	2.20×10^{-4}
ψ_{Nm} (d^{-1})	1.16×10^{-4}	1.51×10^{-4}	9.10×10^{-5}	1.12×10^{-4}	1.19×10^{-4}
ψ_{Pm} (d^{-1})	5.27×10^{-4}	5.23×10^{-4}	5.31×10^{-4}	1.42×10^{-3}	3.56×10^{-4}
r_{DOM} (m^2·g^{-1} N·d^{-1})	2.57×10^{-6}	3.24×10^{-6}	2.09×10^{-6}	2.57×10^{-6}	2.57×10^{-6}
D_{C1} at SS (g C/m^2)	2 970	2 970	2 970	2 970	2 970
D_{N1} at SS (g N/m^2)	130.72	103.67	160.87	130.72	130.72
D_{P1} at SS (g P/m^2)	6.83	6.83	6.83	2.60	9.91
D_{C1} at $t = 0$ (g C/m^2)	3 889.14	3 889.14	3 889.14	3 889.14	3 889.14
D_{N1} at $t = 0$ (g N/m^2)	162.74	135.69	192.89	162.74	162.74
D_{P1} at $t = 0$ (g P/m^2)	13.52	13.52	13.52	9.29	16.60
D_{C2} (g C/m^2)	12 770	12 770	12 770	12 770	12 770
D_{N2} (g N/m^2)	724.18	751.18	694.022	724.18	724.18
D_{P2} (g P/m^2)	47.89	47.89	47.89	52.12	44.81

Notes: Parameters are: ϕ_N, Phase II C:N ratio; ϕ_P, Phase II C:P ratio; α, microbial uptake rate constant; ψ, mineralization constant (ψ_m for C); r_{DOM}, DOM production rate constant; D, soil organic C, N, or P at Phase I (subscript 1) and Phase II (subscript 2) from Table 1. SS indicates steady-state values, and $t = 0$ indicates initial values for simulations of recovery from a bole-only harvest.

N:P ratio for plant uptake, litterfall, and net mineralization equal to 14.94, 15.05, and 15.03 in year 30. However, this synchronization is for the stoichiometry of a young forest and the N:P ratios are therefore ~7% higher than in the steady state. These flux ratios remain high until biomass stops accumulating, at which point N is mineralized in excess of plant needs, the N:P ratio of net mineralization increases while the N:P ratio of uptake and of litterfall decrease, inorganic N builds up in soil solution (Fig. 4b), the ecosystem loses N (Fig. 4a), and the fluxes eventually resynchronize at the steady-state flux ratios.

As with most models where production is constrained by nutrients (e.g., Aber et al. 1982, Seely et al. 2002), our model predicts a decrease in the biomass of the mature ecosystem (age 200 years) following a harvest and the associated loss of nutrient capital. Many of these models are based on interactions between C and N, but not P (e.g., McNeil et al. 2006); the limitation on full biomass recovery in the models is therefore by N and not by a transition from N to P limitation, as in our model. These models also retain a sensitivity to N fertilization (e.g., Currie et al. 1999), whereas ours transitions to P and then to co-limitation. Relative to community-based models like JABOWA (Botkin et al. 1972), our biogeochemical model predicts an earlier peak biomass (~year 120 vs. year 200) and smaller post peak decline in biomass (10% vs. 20–30%; Botkin et al. 1972, Bormann and Likens 1979). Also, unlike these community models, our model eventually converges on the original steady state used for calibration once the N and P lost from the disturbance can be re-accumulated from the slow input fluxes (>1000 years). The MEL model has only two steady states for a given set of environ-mental conditions: the steady state to which the model is calibrated and a state with no vegetation or soil.

The P loss early in the recovery is a key feature of our simulations. It is initiated by the high N:P ratio of our soils relative to the N:P ratio of the post-disturbance residue. Reported soil N:P ratios vary widely, not only because of differences among ecosystems, but also because of methodological differences and difficulties in separating organic from inorganic P. Therefore, reported values might not be directly comparable to our values. With this caveat, our estimate of the soil N:P ratio of 15.6 is not unusually high relative to other studies, which range from 12 to 69 (Sollins et al. 1980, Johnson et al. 1982, Huang and Schoenau 1996, Ross et al. 1999). The N:P ratio of the post-disturbance residue also varies among ecosystems and reflects the N:P of vegetation. Sollins et al. (1980) report an N:P of 6.6 for the mature conifer forest at H. J. Andrews Experimental Forest in Oregon, similar to the 7.4 we use, but Johnson et al. (1982) report a much higher vegetation N:P ratio of 14.3–15.5 for an oak forest at Walker Branch in Tennessee. Clearly, the N:P ratio difference between soil and vegetation is much smaller at Walker Branch than in our simulations and disturbance in this type of forest could result in dynamics that differ from those we describe.

Our sensitivity analyses shed light on the mechanisms underlying the recovery dynamics in our simulations. Again, the key feature in our simulations is the early loss of actively cycling P. However, most of the mechanisms to prevent this loss that we examined only have small effects or actually exacerbated the problem. For example, immobilizing the P into SOM (e.g., by adding C-rich postharvest residue (Fig. 5); fast turnover of woody debris (Fig. 6f); increased immobilization

PLATE 1.   A re-growing northern hardwood forest being fertilized to test some of the ideas presented in this paper. Photo credit: M. A. Vadeboncoeur.

potential (Fig. 7f); or redistributing P between slow and fast turnover SOM (Fig. 8f)) either is stoichiometrically constrained by microbial requirements for N or increases competition with plants for nutrients in general and exacerbates the P loss in the long term. Immobilization of P into plant biomass (e.g., by planting biomass; Fig. 6f) is also constrained stoichiometrically and therefore does not work unless the plants have a ready supply of N.

Buffering of PO_4^{3-} concentration does have a pronounced effect on P retention and the long-term C recovery in our simulations. Buffering is effective because it is not constrained stoichiometrically and it does not compete with vegetation by lowering PO_4^{3-} to limiting concentrations. The buffering in our model is based on instantaneous PO_4^{3-} sorption–desorption on soil particles. The same long-term effect on ecosystem C and nutrient budgets could also be achieved by any P-sequestering reaction that is not stoichiometrically constrained and releases PO_4^{3-} back into soil solution on a time scale of decades or quicker. For example, the formation and weathering of non-occluded P minerals might fit this role if they could form fast enough to avoid the large P loss between years 10 and 30, and could release PO_4^{3-} fast enough to meet biotic demand thereafter. Buffering NH_4^+ concentration does not have an effect on long-term C recovery because the major loss of N occurs as the ecosystem approaches the peak of the C recovery curve, a peak that is set by P limitation.

Fertilization with NH_4^+ has a significant effect on C recovery if the fertilizer is added within 20 years of the harvest. By adding N early in the recovery, when plants are N limited, vegetation accumulates rapidly, sequesters P in biomass, and thereby retains P in the active ecosystem cycle. Although not included in our simulations, both symbiotic and asymbiotic N fixation early in succession might serve the same function (Vitousek et al. 2002). Between years 30 and 100 of the recovery, our simulations indicate that the ecosystem will be more responsive to PO_4^{3-} fertilization because it replaces P lost earlier. Blum et al. (2002) suggest that mycorrhizal assemblages are capable of accelerating apatite weathering, which could serve as a P analogue to N fixation during this phase of the recovery. After the vegetation reaches peak biomass, plants and microbes are able to optimize resource acquisition without having to constantly adjust to a rapidly changing environment and our simulations indicate that co-limitation should prevail.

The transition to P limitation and then to co-limitation in our simulations does not fit the long-held paradigm of N limitation in temperate forests (Vitousek and Howarth 1991, LeBauer and Treseder 2008, Finzi 2009). Exceptions to this paradigm are based on high N inputs or P losses by long-term soil weathering (Aber et al. 1989, Richardson et al. 2004, Gradowski and Thomas 2006, Lambers et al. 2008, Vitousek et al. 2010). However, the paradigm itself is now being questioned (Davidson and Howarth 2007, Elser et al. 2007). For example, Naples and Fisk (2010) used root in-growth cores amended with N, P, or calcium (Ca) to assess limitation at Hubbard Brook and nearby Bartlett

Forest. A mature stand at Hubbard Brook responded only to Ca, but at Bartlett the response is consistent with P limitation in mid succession and N–P co-limitation in late succession. Elser et al. (2007) and Vadeboncoeur (2010), in large meta-analyses, found evidence for N as well as P limitation and showed that many, if not most, ecosystems are co-limited. A transition to co-limitation at steady state is the central prediction of the Resource Optimization Paradigm (Bloom et al. 1985, Chapin et al. 1987) and is at the heart of the MEL model used in this study. However, our simulations indicate that co-limitation cannot fully develop until the N and P cycles resynchronize following disturbance, which took more than 100 years in our simulations.

It is also difficult to compare stream-water losses to our simulated losses because we do not simulate the retention and processing of materials in the vadose zone, ground water, riparian areas, and streams (Newbold et al. 1981, 1982, Hedin et al. 1998, Kroeger 2003). Nevertheless, Martin et al. (2000) report a cumulative stream-water NO_3^- loss over 14 years that is 5.4 g N/m^2 higher from a watershed subjected to a whole-tree harvest (Hubbard Brook watershed 5) than from a control watershed (watershed 6). The gross loss of N over 14 years in our simulation of recovery from a whole-tree harvest is 7 g N/m^2 through leaching of NH_4^+, NO_3^-, and DON, and 26.1 g N/m^2 through denitrification; the comparable numbers for our mature forest are, respectively, 5.2 and 9.1 g N/m^2 (Table 2; total input over 14 years = 14.3 g N/m^2). Thus our simulations indicate an increase in N leaching losses of only 1.8 g N/m^2 over 14 years, but an increase in denitrification of 17 g N/m^2; a 20% redistribution of N loss from denitrification to leaching would bring our leaching loss number into agreement with Martin et al. (2000). When compared in terms of a percentage change in leaching losses with a whole-tree harvest relative to the control, the Martin et al. (2000) data indicate a 27% increase in stream-water NO_3^- loss over 14 years, and our simulations indicate a 35% increase in leaching losses of N.

Comparison of our simulation results to stream-water losses is even more difficult for P because PO_4^{3-} is adsorbed so strongly to soils. Hobbie and Likens (1973) report stream-water PO_4^{3-} losses from a watershed in which all vegetation was cut, the cut biomass was left on site, and the site was treated with herbicides to prevent vegetation recovery (Likens et al. 1970; Watershed 2). Three years after the vegetation was cut, the watershed lost 0.02 g $P \cdot m^{-2} \cdot yr^{-1}$ in steam water. To simulate similar conditions, we reran the hurricane blowdown simulation, but did not allow the vegetation to regrow. Losses from all the soil organic pools plus soil PO_4^{3-} are over an order of magnitude higher (0.35 g $P \cdot m^{-2} \cdot yr^{-1}$) in our simulations than those reported by Hobbie and Likens (1973). However, >73% of that P loss accumulated in secondary minerals within the rooting zone in the model (i.e., in P_{2nd}); the remaining 27% leached out

of the rooting zone as PO_4^{3-}. A large fraction of this leaching loss would likely be adsorbed onto soil particles below the rooting zone and therefore would not be detected in the stream water.

Our simulations provide a heuristic perspective that should provide guidance for future research and, if corroborated by observation, provide guidance for forest management. The most surprising hypothesis suggested from our model analysis is that the stoichiometric discrepancy between post-disturbance residue and soil organic matter should result in the preferential loss of P and retention of N by the ecosystem. This hypothesis should be testable and our simulations indicate that the effects should be detectable within 5–30 years. If the hypothesis is falsified, then the mechanism for retaining or replacing P should be identified. If corroborated, our simulations suggest a management scheme of N fertilization after the vegetation becomes established but before canopy closure (fertilize between years 10 and 30); fertilization with N during this period should stimulate plant growth and help to sequester both N and P in biomass and thereby avoid a loss of P that is difficult to recover. Increasing anion sorption capacity during this period might also be effective at retaining PO_4^{3-}. After canopy closure and before peak biomass, P fertilization should be more effective than N fertilization. In older forests, our simulations indicate co-limitation and the forest should be most responsive to a stoichiometrically balanced fertilizer.

Literature Cited

Aber, J. D., J. M. Melillo, and C. A. Federer. 1982. Predicting the effects of rotation length, harvest intensity, and fertilization on fiber yield from northern hardwood forests in New England. Forest Science 28:31–45.

Aber, J. D., K. J. Nadelhoffer, P. Steudler, and J. M. Melillo. 1989. Nitrogen saturation in northern forest ecosystems. BioScience 39:378–386.

Acker, M. 2006. Base cation concentration and content in litterfall and woody debris across a northern hardwood forest chronosequence. Thesis. University of Kentucky, Lexington, Kentucky, USA.

Alban, D. H., and J. Pastor. 1993. Decomposition of aspen, spruce, and pine boles on two sites in Minnesota. Canadian Journal of Forest Research 23:1744–1749.

Bailey, A. S., J. W. Hornbeck, J. L. Campbell, and C. Eagar. 2003. Hydrometeorology database for Hubbard Brook Experimental Forest: 1955–2000. USDA Forest Service General Technical Report NE-303, Newton Square, Pennsylvania, USA.

Beisner, B. E., D. T. Haydon, and K. Cuddington. 2003. Alternative stable states in ecology. Frontiers in Ecology and the Environment 1:376–382.

Bernal, S., L. O. Hedin, G. E. Likens, S. Gerber, and D. C. Buso. 2012. Complex response of the forest nitrogen cycle to

climate change. Proceedings of the National Academy of Sciences USA 109:3406–3411.

Bloom, A. J., F. S. Chapin, III, and H. A. Mooney. 1985. Resource limitation in plants—an economic analogy. Annual Review of Systematics and Ecology 16:363–392.

Blum, J. D., A. Klaue, C. A. Nezat, C. T. Driscoll, C. E. Johnson, T. G. Siccama, C. Eager, T. J. Fahey, and G. E. Likens. 2002. Mycorrhizal weathering of apatite as an important calcium source in base-poor forest ecosystems. Nature 417:729–731.

Booth, M. S., J. M. Stark, and E. B. Rastetter. 2005. Controls on nitrogen cycling in terrestrial ecosystems: a synthetic analysis of literature data. Ecological Monographs 75:139–157.

Bormann, F. H., and G. E. Likens. 1979. Catastrophic disturbance and the steady state in northern hardwood forests: A new look at the role of disturbance in the development of forest ecosystems suggests important implications for land-use policies. American Scientist 67:660–669.

Botkin, D. B., J. F. Janak, and J. R. Wallis. 1972. Some ecological consequences of a computer model of forest growth. Journal of Ecology 60:849–872.

Brubaker, K., A. Rango, and W. Kustas. 1996. Incorporating radiation inputs into the snowmelt runoff model. Hydrological Processes 10:1329–1343.

Buso, D. C., G. E. Likens, and J. S. Eaton. 2000. Chemistry of precipitation, streamwater, and lakewater from the Hubbard Brook ecosystem study: a record of sampling protocols and analytical procedures. USDA Forest Service General Technical Report NE-275, Newton Square, Pennsylvania, USA.

Chapin, F. S., III, A. J. Bloom, C. B. Field, and R. H. Waring. 1987. Plant responses to multiple environmental factors. BioScience 37:49–57.

Clapp, R. B., and G. M. Hornberger. 1978. Empirical equations for soil hydraulic properties. Water Resources Research 14:601–604.

Covington, W. W., and J. D. Aber. 1980. Leaf production during secondary succession in northern hardwoods. Ecology 61:200–204.

Crews, T. E., K. Kitayama, J. H. Fownes, R. H. Riley, D. A. Herbert, D. Mueller-Dombois, and P. M. Vitousek. 1995. Changes in soil phosphorus fractions and ecosystems dynamics across a long chronosequence in Hawaii. Ecology 76:1407–1424.

Currie, W. S., J. D. Aber, W. H. McDowell, R. D. Boone, and A. H. Magill. 1996. Vertical transport of dissolved organic C and N under long-term N amendments in pine and hardwood forests. Biogeochemistry 35:471–505.

Currie, W. S., K. J. Nadelhoffer, and J. D. Aber. 1999. Soil detrital processes controlling the movement of ^{15}N tracers to forest vegetation. Ecological Applications 9:87–102.

Davidson, E., and R. W. Howarth. 2007. Nutrients in synergy. Nature 449:1000–1001.

Dittman, J. A., C. T. Driscoll, P. M. Groffman, and T. J. Fahey. 2007. Dynamics of nitrogen and dissolved organic carbon at the Hubbard Brook Experimental Forest. Ecology 88:1153–1166.

Elser, J. J., M. E. S. Bracken, E. E. Cleland, D. S. Gruner, W. S. Harpole, H. Hillebrand, J. T. Ngai, E. W. Seabloom, J. B. Shurin, and J. E. Smith. 2007. Global analysis of nitrogen and phosphorus limitation of primary producers in freshwater, marine and terrestrial ecosystems. Ecology Letters 10:1135–1142.

Fahey, T. J., J. W. Hughes, M. Pu, and M. A. Arthur. 1988. Root decomposition and nutrient flux following whole-tree harvest of northern hardwood forest. Forest Science 34:744–768.

Fahey, T. J., et al. 2005. The biogeochemistry of carbon at Hubbard Brook. Biogeochemistry 75:109–176.

Finzi, A. C. 2009. Decades of atmospheric deposition have not resulted in widespread phosphorus limitation or saturation of tree demand for nitrogen in southern New England. Biogeochemistry 92:217–229.

Gradowski, T., and S. C. Thomas. 2006. Phosphorus limitation of sugar maple growth in central Ontario. Forest Ecology and Management 226:104–109.

Groffman, P. M., C. T. Driscoll, T. J. Fahey, J. P. Hardy, R. D. Fitzhugh, and G. L. Tierney. 2001. Effects of mild winter freezing on soil nitrogen and carbon dynamics in a northern hardwood forest. Biogeochemistry 56:191–213.

Hedin, L. O., J. C. von Fischer, N. E. Ostrom, B. P. Kennedy, M. G. Brown, and G. P. Robertson. 1998. Thermodynamic constraints on nitrogen transformations and other biogeochemical processes at soil–stream interfaces. Ecology 79:684–703.

Hobbie, J. E., and G. E. Likens. 1973. Output of phosphorus, dissolved organic C and fine particulate carbon from Hubbard Brook Watersheds. Limnology and Oceanography 18:734–742.

Houghton, R. A., J. E. Hobbie, J. M. Melillo, B. Moore, B. J. Peterson, G. R. Shaver, and G. M. Woodwell. 1983. Changes in the carbon content of terrestrial biota and soils between 1860 and 1980: A net release of CO_2 to the atmosphere. Ecological Monographs 53:235–262.

Huang, W. Z., and J. J. Schoenau. 1996. Forms, amounts, and distribution of carbon, nitrogen, phosphorus, and sulfur in a boreal aspen forest soil. Canadian Journal of Soil Science 76:373–385.

Hyvönen, R., and G. I. Ågren. 2001. Decomposer invasion rate, decomposer growth rate, and substrate chemical quality: how they influence soil organic matter turnover. Canadian Journal of Forest Research 31:1594–1601.

Johnson, D. W., D. C. West, D. E. Todd, and L. K. Mann. 1982. Effects of sawlog vs. whole-tree harvesting on the nitrogen, phosphorus, potassium, and calcium budgets of an upland mixed oak forest. Soil Science Society of America Journal 46:1304–1309.

Kaiser, K., and W. Zech. 1996. Nitrate, sulfate, and biphosphate retention in acid forest soils affected by natural dissolved organic carbon. Journal of Environmental Quality 25:1325–1331.

Kroeger, K. D. 2003. Controls on magnitude and species composition of groundwater-transported nitrogen exports from glacial outwash plain watersheds. Dissertation. Boston University, Boston, Massachusetts, USA.

Lambers, H., J. A. Raven, G. Shaver, and S. E. Smith. 2008. Plant nutrient-acquisition strategies change with soil age. Trends in Ecology and Evolution 23:95–103.

LeBauer, D. S., and K. K. Treseder. 2008. Nitrogen limitation of net primary productivity in terrestrial ecosystems is globally distributed. Ecology 89:371–379.

Leonard, R. E. 1961. Net precipitation in a northern hardwood forest. Journal of Geophysical Research 66:2417–2421.

Likens, G. E., and F. H. Bormann. 1995. Biogeochemistry of a forested ecosystem. Springer-Verlag, New York, New York, USA.

Likens, G. E., F. H. Bormann, N. M. Johnson, D. W. Fisher, and R. S. Pierce. 1970. Effects of forest cutting and herbicide treatment on nutrient budgets in the Hubbard Brook watershed-ecosystem. Ecological Monographs 40:23–47.

Lovett, G. M., J. J. Bowser, and E. S. Edgerton. 1997. Atmospheric deposition to watersheds in complex terrain. Hydrological Processes 11:645–654.

Marks, P. L., and F. H. Bormann. 1972. Revegetation following forest cutting: mechanisms for return to steady-state nutrient cycling. Science 176:914–915.

Martin, C. W., J. W. Hornbeck, G. E. Likens, and D. C. Buso. 2000. Impacts of intensive harvesting on hydrology and nutrient dynamics of northern hardwood forests. Canadian Journal of Fisheries and Aquatic Sciences 57 (Supplement 2):19–29.

Mattson, K. G., W. T. Swank, and J. B. Waide. 1987. Decomposition of woody debris in a regenerating, clear-cut forest in the Southern Appalachians. Canadian Journal of Forest Research 17:712–721.

May, R. M. 1977. Thresholds and breakpoints in ecosystems with a multiplicity of states. Nature 269:471–477.

McNeil, B. E., R. E. Martell, and J. M. Read. 2006. GIS and biogeochemical models for examining the legacy of forest disturbance in the Adirondack Park, NY, USA. Ecological Modelling 195:281–295.

Melillo, J. M., J. D. Aber, A. E. Linkins, A. Ricca, B. Fry, and K. J. Nadelhoffer. 1989. Carbon and nitrogen dynamics along the decay continuum: Plant litter to soil organic matter. Plant and Soil 115:189–198.

Mikolajkow, J. 2003. Laboratory methods of estimating the retardation factor of migrating mineral nitrogen compounds in shallow groundwater. Geological Quarterly 47:91–96.

Nadelhoffer, K. J., B. A. Emmett, P. Gundersen, O. J. Kjonaas, C. J. Koopmans, P. Schleppi, A. Tietema, and R. F. Wright. 1999. Nitrogen deposition makes a minor contribution to carbon sequestration in temperate forests. Nature 398:145–148.

Naples, B. K., and M. C. Fisk. 2010. Belowground insights into nutrient limitation in northern hardwood forests. Biogeochemistry 97:109–121.

Newbold, J. D., J. W. Elwood, R. V. O'Neill, and W. Van Winkle. 1981. Measuring nutrient spiraling in streams. Canadian Journal of Fisheries and Aquatic Science 38:860–863.

Newbold, J. D., R. V. O'Neill, J. W. Elwood, and W. Van Winkle. 1982. Nutrient spiraling in streams: implications for nutrient limitation and invertebrate activity. American Naturalist 120:628–652.

Nodvin, S. C., C. T. Driscoll, and G. E. Likens. 1986. Simple partitioning of anions and dissolved organic carbon in a forest soil. Soil Science 142:27–35.

Ollinger, S. V., J. D. Aber, G. M. Lovett, S. E. Millham, R. G. Lathrop, and J. M. Ellis. 1993. A spatial model of atmospheric deposition for the northeastern U.S. Ecological Applications 3:459–472.

Rastetter, E. B. 2011. Modeling coupled biogeochemical cycles. Frontiers in Ecology and the Environment 9:68–73.

Rastetter, E. B., G. I. Ågren, and G. R. Shaver. 1997. Responses of N-limited ecosystems to increased CO_2: a balanced-nutrition, coupled-element-cycles model. Ecological Applications 7:444–460.

Rastetter, E. B., P. M. Vitousek, C. Field, G. R. Shaver, D. Herbert, and G. I. Ågren. 2001. Resource optimization and symbiotic N fixation. Ecosystems 4:369–388.

Redfield, A. C. 1958. The biological control of chemical factors in the environment. American Scientist 46:205–221.

Richardson, S. J., D. A. Peltzer, R. B. Allen, M. S. McGlone, and R. L. Parfitt. 2004. Rapid development of phosphorus limitation in temperate rainforest along the Franz Josef soil chronosequence. Oecologia 139:267–276.

Ross, D. J., K. R. Tate, N. A. Scott, and C. W. Feltham. 1999. Land-use change: effects on soil carbon, nitrogen, and phosphorus pools and fluxes in three adjacent ecosystems. Soil Biology and Biochemistry 31:803–813.

Schimel, J. P., and M. N. Weintraub. 2003. The implications of exoenzyme activity on microbial carbon and nitrogen limitation in soil: a theoretical model. Soil Biology and Biochemistry 35:549–563.

Seely, B., C. Welham, and H. Kimmins. 2002. Carbon sequestration in a boreal forest ecosystem: Results from the ecosystem simulation model, FORECAST. Forest Ecology and Management 169:123–135.

Sollins, P., C. C. Grier, F. M. McCorison, K. Cromack, Jr, R. Fogel, and R. L. Fredricksen. 1980. The internal element cycles of an old-growth Douglas-fir ecosystem in Western Oregon. Ecological Monographs 50:261–285.

Vadeboncoeur, M. A. 2010. Meta-analysis of fertilization experiments indicates multiple limiting nutrients in northeastern deciduous forests. Canadian Journal of Forest Research 40:1766–1780.

Vandenbruwane, J., S. D. Neve, R. G. Qualls, S. Sleutel, and G. Hofman. 2007. Comparison of different isotherm models for dissolved organic carbon (DOC) and nitrogen (DON) sorption to mineral soil. Geoderma 139:144–153.

Vitousek, P. M., K. Cassman, C. Cleveland, T. Crews, C. B. Field, N. Grimm, R. W. Howarth, R. Marino, L. Martinelli, E. B. Rastetter, and J. Sprent. 2002. Towards an ecological understanding of biological nitrogen fixation. Biogeochemistry 57/58:1–45.

Vitousek, P. M., and R. W. Howarth. 1991. Nitrogen limitation on land and in the sea: how can it occur? Biogeochemistry 13:87–115.

Vitousek, P. M., S. Porder, B. Z. Houlton, and O. A. Chadwick. 2010. Terrestrial phosphorus limitation: mechanisms, implications, and nitrogen–phosphorus interactions. Ecological Applications 20:5–15.

Waring, R. H., and W. H. Schlesinger. 1985. Forest ecosystems: concepts and management. Academic Press, Orlando, Florida, USA.

Weatherley, L. R., and N. D. Miladinovic. 2004. Comparison of the ion exchange uptake of ammonium ion onto New Zealand clinoptilolite and mordenite. Water Research 38:4305–4312.

Whittaker, R. H., G. E. Likens, F. H. Bormann, J. S. Eaton, and T. G. Siccama. 1979. The Hubbard Brook ecosystem study: forest nutrient cycling and element behavior. Ecology 60:203–220.

Yanai, R. D. 1992. Phosphorus budget of a 70-year-old northern hardwood forest. Biogeochemistry 17:1–22.

Yanai, R. D. 1998. The effect of whole-tree harvest on phosphorus cycling in a northern hardwood forest. Forest Ecology and Management 104:281–295.

Yanai, R. D., W. S. Currie, and C. L. Goodale. 2003. Soil carbon dynamics after forest harvest: an ecosystem paradigm reconsidered. Ecosystems 6:197–212.

Supplemental Material

Appendix

Tables presenting equations for the multiple element limitation (MEL) model and the process and parameter definitions, values, and sources for the MEL model (*Ecological Archives* A023-029-A1).